UNIVERSITY OF CALIFORNIA SAN DIEGO

Identification and Characterization of a Sodium/Hydrogen Exchanger in the Coral Species *Acropora yongei*: a potential role in biomineralization.

A Thesis submitted in partial satisfaction of the requirements for the degree Master of Science

in

Marine Biology

by

Mikayla Janeice Ortega

Committee in charge:

Martin Tresguerres, Chair
Eric Allen
David Kline
Jennifer Taylor

2018

The Thesis of Mikayla Janeice Ortega is approved and it is acceptable in quality and form for publication on microfilm and electronically:

_____

_____

_____

_____

Chair

University of California San Diego

2018

DEDICATION

I dedicate this thesis to my family, friends, lab-mates and colleagues. I am particularly thankful to my parents, Tony and Michelle Ortega, for their unconditional love, support and encouragement throughout this process and all of the adventures I choose to pursue in life; my three sisters, Emily, Lilly, and Bethany, who inspire me daily to be a better person and scientist through their constant faith and belief in me. I also give special thanks to my friends for their cheer, reassurance, and constant provision of caffeine throughout this challenging season of life. Thank you for all the memories we have made and reminding me that sun breaks are important and snacks are always necessary.

Additionally, I want to thank all the members of the Tresguerres Lab for their guidance and support in research and in life- Dr. Martin Tresguerres for his encouragement, challenge, and mentorship; thank you for shaping me into the scientist I am. To Dr. Jinae Roa, thank you for giving me my start in research, providing me a solid foundation, and for your constant encouragement and belief in me that I have what it takes. To the rest of the Tresguerres Lab, thank you for celebrating with me in times of success and brainstorming in times of struggle; thank you for your constant support and for the reminder that academic life is about having a balance. I will always cherish the laughs and memories we've shared in and out of lab.

EPIGRAPH

She believed she could, so she did.

Unknown

I have not failed. I've successfully discovered 10,000 things that won't work.

Thomas Edison

Research is what I'm doing when I don't know what I'm doing.

Wernher von Braun

TABLE OF CONTENTS

LIST OF ABBREVIATIONS

ACC	Amorphous calcium carbonate
BHH	Benzamidine hydrochloride hydrate
BSA	Boving serum albinum
$CaCO_3$	Calcium carbonate
CARPs	Coral acid-rich proteins
CCM	Carbon concentrating mechanism
CPA	Cation proton antiporter gene superfamily
DIC	Dissolved inorganic carbon; CO_2, HCO_3^-, and CO_3^{2-}
DTT	Dithiothreitol
GFP	Green fluorescent protein
$[H^+]$	Concentration of proton/hydrogen ion/acid molecule
$[Na^+]$	Concentration of sodium ions
NaT-DC	Sodium-transporting carboxylic decarboxylase gene superfamily
NHA	Sodium-Hydrogen Antiporter
NHE	Sodium-Hydrogen Exchanger (Na^+-H^+ Exchanger)
NKA	Sodium-Potassium ATPase (Na^+-K^+-ATPase)
OA	Ocean acidification
PBS	Phosphate buffered saline
PBS-T	Phosphate buffered saline, 0.2% Triton-X
PMSF	Phenylmethylsulfonyl fluoride
pHe	Extracellular pH
pHi	Intracellular pH
SCM	Subcalicoblastic medium
SLC9	Solute carrier transporter 9
SOM	Skeletal organic matrix
TBS-T	Tris-buffered saline and 0.1% Tween detergent
VHA	Vacuolar-type Proton-ATPase (H^+-ATPase)

LIST OF FIGURES

LIST OF TABLES

ACKNOWLEDGEMENTS

This work was funded by the National Science Foundation (NSF) Ocean Sciences #1538495 and Emerging Frontiers #1220641.

I would like to acknowledge Dr. Jennifer Taylor, Dr. Eric Allen, and Dr. David Kline for serving on my thesis committee. I am deeply appreciative of your time and support of my Master's thesis.

I would also like to give special acknowledgement to Phil Zerofski for all he does in helping us take care of our coral and maintaining our coral tanks; to Andreas Andersson for his assistance and guidance throughout my degree.

This thesis is being prepared for submission for publication of the material. Ortega, Mikayla; Tresguerres, Martin. Ms. Ortega was the primary investigator and author of this material.

ABSTRACT OF THE THESIS

Identification and Characterization of a Sodium/Hydrogen Exchanger in the Coral Species *Acropora yongei*: a potential role in biomineralization.

by

Mikayla Janeice Ortega

Master of Science in Marine Biology

University of California San Diego, 2018

Dr. Martin Tresguerres, Chair

Coral biomineralization is an important physiological process responsible for creating the massive reef ecosystems found throughout the world. Biomineralization requires the transport of Ca^{2+} and dissolved inorganic carbon (DIC) to the subcalicoblastic medium (SCM), which is the alkaline microenvironment located underneath coral tissues where the skeleton is built. Additionally, H^{+} are constantly produced as a byproduct of calcification and must be removed from the SCM to prevent acidification that would impede biomineralization, however, the coral cellular mechanisms that perform these processes are mostly unknown. The solute carrier

transporter 9 gene family (*SLC9*) transports Na^+ in exchange for H^+ across a cellular membrane. It is found throughout the animal kingdom to be essential for pH regulation and acid/base homeostasis. For the first time, an SLC9 protein has been characterized in corals. In the coral *Acropora yongei*, this SLC9 protein is found to share the strongest homology with the Na^+/H^+ exchangers (NHEs) 1-5 and potentially experiences post-translational modifications, such as glycosylation and phosphorylation. Specific anti-*Acropora*NHE antibodies were developed and validated, which allowed investigation of protein abundance and cellular localization in coral tissues. Immunolocalization analysis of *Acropora*NHE revealed it to be highly abundant in the calicoblastic cells that secrete skeleton. *Acropora*NHE also localizes to desmocytes, intracellular structures within symbiocyte cells, and the apical membrane of oral ectodermal cells. The presence of NHE in the calicoblastic cells suggests its involvement in intracellular pH regulation, as well as in removing H^+ from the SCM. Future work is needed to confirm the physiological functions of *Acropora*NHE.

INTRODUCTION

Coral reefs are areas of extremely high marine biodiversity, making them important ecosystems to preserve and protect (Carpenter et al., 2008; Moberg & Folke, 1999; Smith, 1978). They constitute ~0.17% of the world ocean's area and cover ~15% of the shallow sea floor (Smith, 1978). Coral reefs provide local and worldwide ecological goods and services (Moberg & Folke, 1999) Ecological goods are the materials people can obtain from an ecosystem, while ecological services are the anthropogenic benefit an ecosystem provides (Beaumont et al., 2007). Coral reefs house about a third of the world's marine fish species, as well as serve as an important source for the global fisheries market (Smith, 1978). They provide material and products important for the pharmaceutical industry, medical research and the construction industry world-wide (Sorokin, 1993; Carté, 1996; Birkeland, 1997). They also protect coastlines from currents, waves, and storm action, which causes erosion that leads to land loss (Moberg & Folke, 1999). Dead coral skeletons become the white sand characteristic of many island beaches, a notable attraction for beach tourists (Moberg & Folke, 1999; Richmond, 1993), and coral reefs support recreational activities that greatly contribute to the tourism economy (Dixon et al., 1993; Pendleton, 1995; Cesar, 1996). In 1990, Caribbean tourism was worth US$8.9 billion and employed over 350,000 people (Dixon et al., 1993).

Additionally, coral reefs provide multiple biological services by functioning as important breeding, spawning, nursery, and feeding grounds for a variety of organisms (Moberg & Folke, 1999). The extensive bacterial community hosted by corals plays an important role in nitrogen fixation, providing a limiting nutrient in a bioavailable form that allows diverse organisms to flourish in otherwise uninhabitable waters (Sorokin, 1993). The skeletons of reef-building corals and various other reef organisms can provide historical information on oceanic conditions, as

well as past and present changes due to anthropogenic effects on the marine environment (Eisenhauer et al., 1993; Runnalls & Coleman, 2003), especially when studied as long-term chemical recorders for various seawater constituents (Dodge & Gilbert, 1984; Howard & Brown, 1984; Wilkinson, 1993; Eakin et al., 1997).

Despite the biological and economic importance of corals, very little is known about their physiology at the cellular and molecular level. Though corals are considered simple animals evolutionarily and by body plan standards, they are actually rather complex. They contain a large diversity of cell types that are specialized for specific physiological functions and have developed symbioses with various other organisms to meet otherwise unattainable physiological needs. Since very little is known about coral cell physiology, further elucidation of coral cellular functions can increase our understanding of how corals respond to environmental and anthropogenic stress, potentially informing coral conservation and management strategies. The focus of my thesis is to investigate and identify cellular physiological mechanisms involved in acid/base homeostasis and calcification.

Coral Anatomy

Corals belong to the phylum Cnidaria (Class Anthozoa, Subclass Hexacorallia, Order Scleratinia) (Bourne, 1900). Reef-building corals, also known as stony or hermatypic corals, are responsible for the building of extensive tropical reef ecosystems through the formation of calcium carbonate ($CaCO_3$) skeletons beneath their tissues (Burke et al., 2011). Reef-building corals are further categorized into two clades, Robust and Complex, which diverged from each other approximately 300 to 400 million years ago, and can be distinguished by differences in their skeletal structure and modes of asexual growth (Romano & Palumbi, 1996; Romano &

Cairns, 2000; Stolarski et al., 2011). Corals of the Robust clade tend to have more heavily calcified skeletons and use intratentacular budding, where a parent corallite splits down the middle to form a daughter corallite (Wijsman-Best, 1977). The Complex clade is characterized by having a more porous skeleton and uses extratentacular budding for asexual growth, where production of a daughter corallite is external to the wall of the parent corallite (Wijsman-Best, 1977). The common ancestor of Robust and Complex corals lacked a $CaCO_3$ skeleton, suggesting that calcification evolved independently in the two coral clades and, therefore, the cellular mechanisms involved in calcification can not be assumed to be the same amongst all coral species (Romano & Palumbi, 1996).

An individual coral animal referred to as a polyp. Corals are colonial animals that can contain hundreds of polyps that are all connected by the coenosarc (the tissue between the polyps), and the coelenteron (also known as the gastrovascular cavity), which circulates fluid throughout the colony (Figure 1A). Like all Cnidarians, corals are diploblastic, meaning they have two tissue types: the ectoderm and endoderm. After fertilization and embryo development, coral larvae settle onto a hard substrate with the mouth, or oral pole, facing upward and the aboral pole attached to the substrate. Both oral and aboral tissues then differentiate into an ectodermal and an endodermal layer, leading to four total tissue layers in the adult coral colony (Figure 1A). The ectoderm and endoderm are connected by mesoglea, an extracellular matrix of connective proteic fibers and water (Phillips, 1963) (Figure 1B). The oral layers are located above the coelenteron and the aboral layers are located below (Figure 1B). The oral ectoderm interacts with seawater, the aboral ectoderm with the skeleton, and both endodermal layers, referred to as the gastrodermal layers, line the coelenteron. Each of these tissue layers has a variety of specialized cell types, adding complexity to coral anatomy.

Figure 1. Coral Colony and Tissue Anatomy. A) Polyps and coenosarc region of a coral colony, and tissue layer organization into oral ecto- and gastroderm and aboral ecto- and gastroderm. Modified from Tresguerres et al. (2017). B) Detail of the tissue layers: oral ectoderm, oral gastroderm, coelenteron, aboral gastroderm, aboral ectoderm/calicodermis, mesoglea, subcalicoblastic medium (SCM), and skeleton. Modified from Allemand et al. (2011)

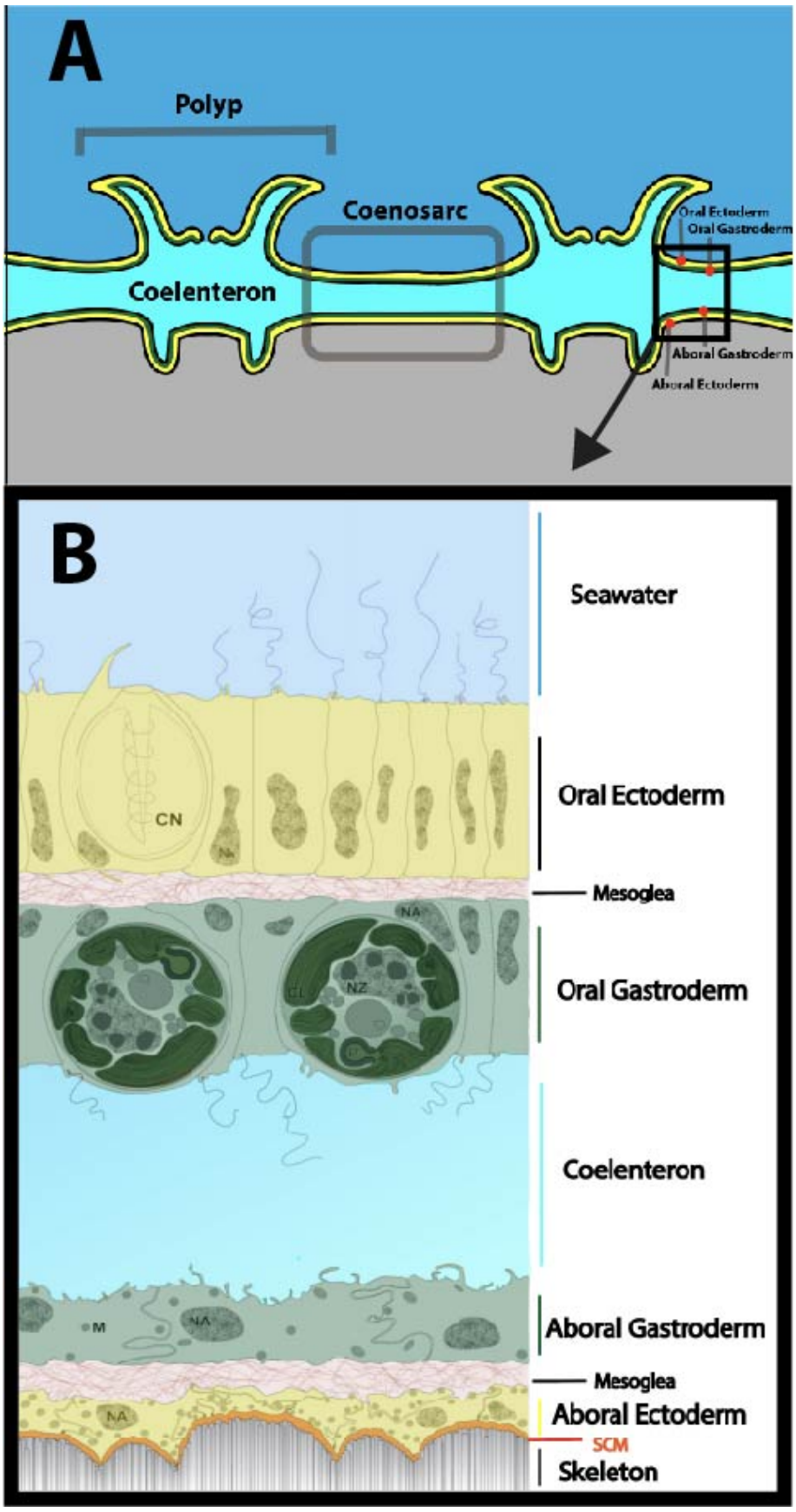
A
Polyp
Coenosarc
Coelenteron
Oral Ectoderm
Oral Gastroderm
Aboral Gastroderm
Aboral Ectoderm
B
Seawater
CN
Oral Ectoderm
Mesoglea
NA
NZ
Oral Gastroderm
Coelenteron
M
NA
Aboral Gastroderm
Mesoglea
NA
Aboral Ectoderm
SCM
Skeleton

The oral ectoderm contains at least six cell types: ciliated support cells with a high abundance of microvilli, cnidoctyes containing nematocysts (stinging cells), mucocytes, pigment cells, neurons, and epithelial muscular cells (Goldberg, 2002). The abundance of each cell type depends on the coral species, the location of polyps within the colony, and the environmental conditions experienced on the reef. Ciliated cells are believed to be involved in ion and nutrient uptake from the seawater and interact with the diverse bacterial community living within the mucus and boundary layer directly above the coral tissue (reviewed in Tresguerres et al., 2017). Additionally, some coral species contain endosymbiotic cyanobacteria within their oral tissue layers that are also speculated to play an important role in nitrogen fixation (Lesser et al., 2004). The oral ectodermal tissue around the polyp mouth is modified to form tentacles containing an abundance of cnidocytes, which contain nematocysts that are important in food capture and defense (Galloway et al., 2007; Veron, 1993).

The oral gastroderm is located below the oral ectoderm. Some gastrodermal cells contain endosymbiotic algae and are referred to as symbiocytes (Tresguerres et al., 2017). The algae are dinoflagellates, of the genus *Symbiodinium*, that are taken up from the coelenteron by phagocytosis (Davy et al., 2012). As a result, endosymbiotic *Symbiodinium* are present inside the symbiosome, an intracellular space inside symbiocytes that is surrounded by the coral host-derived symbiosome membrane. These *Symbiodinium* are considered part of the "coral holobiont", which is the term that encompasses the coral animal together with the diverse organisms that live in close association, including the endosymbiotic algae, cyanobacteria, bacteria, archaea, viruses, endolithic algae, and fungi (Wegley et al., 2004). Symbiocytes typically contain one *Symbiodinium*; however, on occasion they can contain up to three.

Gastrodermal cells are further modified within the center of the polyps to form mesenterial filaments important in food digestion and reproduction (Galloway et al., 2007; Veron, 1993).

Separating the oral and aboral gastrodermal layers is the coelenteron that connects all polyps in the coral colony. The coelenteron is filled with fluid that is circulated throughout the colony by the action of flagella and cilia on the gastrodermal cells. While the coelenteron interfaces with seawater at the mouth of polyps, the chemical composition of the coelenteron fluid is very different than seawater. It contains nitrogen species and phosphates at concentration levels 30- to 2,000-fold higher than seawater, as well as bacterial counts up to 100-fold lower than seawater (Agostini et al., 2012). The coelenteron fluid also has lower concentrations of dissolved oxygen and different levels of pH compared to both the seawater and the coral cells (Agostini et al., 2012; Furla et al., 2000). The amounts of dissolved inorganic carbon (DIC) and gases present, as well as the pH values measured within the coelenteron, vary between different species and are strongly affected by processes such as photosynthesis, calcification, metabolism, and food digestion (Furla et al., 2000).

The bottom two coral tissue layers are the aboral gastroderm and aboral ectoderm, which is also referred to as the calicodermis. The functions of the aboral gastroderm have not been extensively studied, however, it likely plays an important role in the transport of ions from the coelenteron to the calicodermis for calcification. Although the aboral gastroderm also has symbiocytes, they tend to be present in lower concentrations compared to the oral gastroderm. The calicodermis is located directly below the aboral gastroderm, to which it is connected by mesoglea, and is directly above the skeleton. The calicodermis contains two cell types: desmocytes, that anchor the coral tissue to the skeleton, and calicoblastic cells that produce $CaCO_3$ skeleton by cellular mechanisms that are not completely understood.

Coral Calcification

Similar to all other organisms that build skeletons, coral calcification is achieved through a biologically controlled process known as biomineralization (Allemand et al., 2011). The cellular and molecular mechanisms involved in coral calcification remain poorly understood; however, there are at least three processes involved: (1) Ca^{2+} and DIC transport to the site of calcification, (2) removal of H^{+} from the site of calcification, and (3) secretion of biomineralizing organic matrix proteins to the site of calcification (Allemand et al., 2004). Importantly, the skeleton of living corals is below the coral tissues and not in contact with the external seawater. The calicodermis and skeleton are separated by pockets of subcalicoblastic medium (SCM), a microenvironment with an alkaline pH that favors DIC in the form of CO_3^{-} and elevates the saturation state of aragonite to 20-30 fold supersaturated in the light and 3-11 fold in the dark (Venn et al., 2011).

Radioisotopic measurement studies have confirmed seawater is the source of Ca^{2+} for skeletal formation (Goreau, 1959). Since the skeleton is isolated from seawater, the molecules necessary for calcification must be transported to the site of skeleton formation through four cell layers, if absorbed from the water column (Figure 2A), or through two cell layers if absorbed from the coelenteron (Figure 2B). The cells in the calicodermis are connected by tight junctions that create a potential paracellular pathway for Ca^{2+} (Barott et al., 2015a). In addition, Ca^{2+} may move through transcellular pathways that involve ion transporting proteins and vesicular transport. For example, L-type voltage-dependent Ca^{2+} channels in the oral ectoderm of *Stylophora pistillata* have been suggested to take up Ca^{2+} from seawater (Figure 2) (Zoccola et al., 1999). Calcification rates were also shown to decrease with pharmacological inhibition of

these channels (Zoccola et al., 1999), yet in other organisms these channels are used primarily in Ca^{2+} homeostasis and signaling (Hosey & Lazdunski, 1988), so the effect might be unspecific.

Another Ca^{2+}-transporting protein suggested to be important for coral calcification is the plasma membrane Ca^{2+}-ATPase (PMCA) (Allemand et al., 2011; Cohen & Holocomb, 2009; Davy et al., 2012; Zoccola et al., 2004). PMCA in the apical membrane of the calicoblastic cells has been proposed to transport Ca^{2+} into the SCM in exchange for H^+ (Al-Horani et al., 2003; Allemand et al., 2011; Marshall, 1996). Not only would PMCAs serve as a source of Ca^{2+}, but they would also be removing H^+ ions away from the SCM, an important function required to maintain the pH of the SCM (Figure2). This model was based on pharmacological inhibition studies using ruthenium red (Al-Horani et al., 2003), as well as the localization of PMCA mRNA to the calicoblastic cells of *S. pistillata* (Zoccola et al., 2004). However, PMCA mRNA was also abundantly present in gastrodermal cells, and more recent studies found PMCA protein to be cytoplasmic in coral calicoblastic cells rather than in the apical membrane (Barott et al., 2015a), casting doubts about this proposed mechanism.

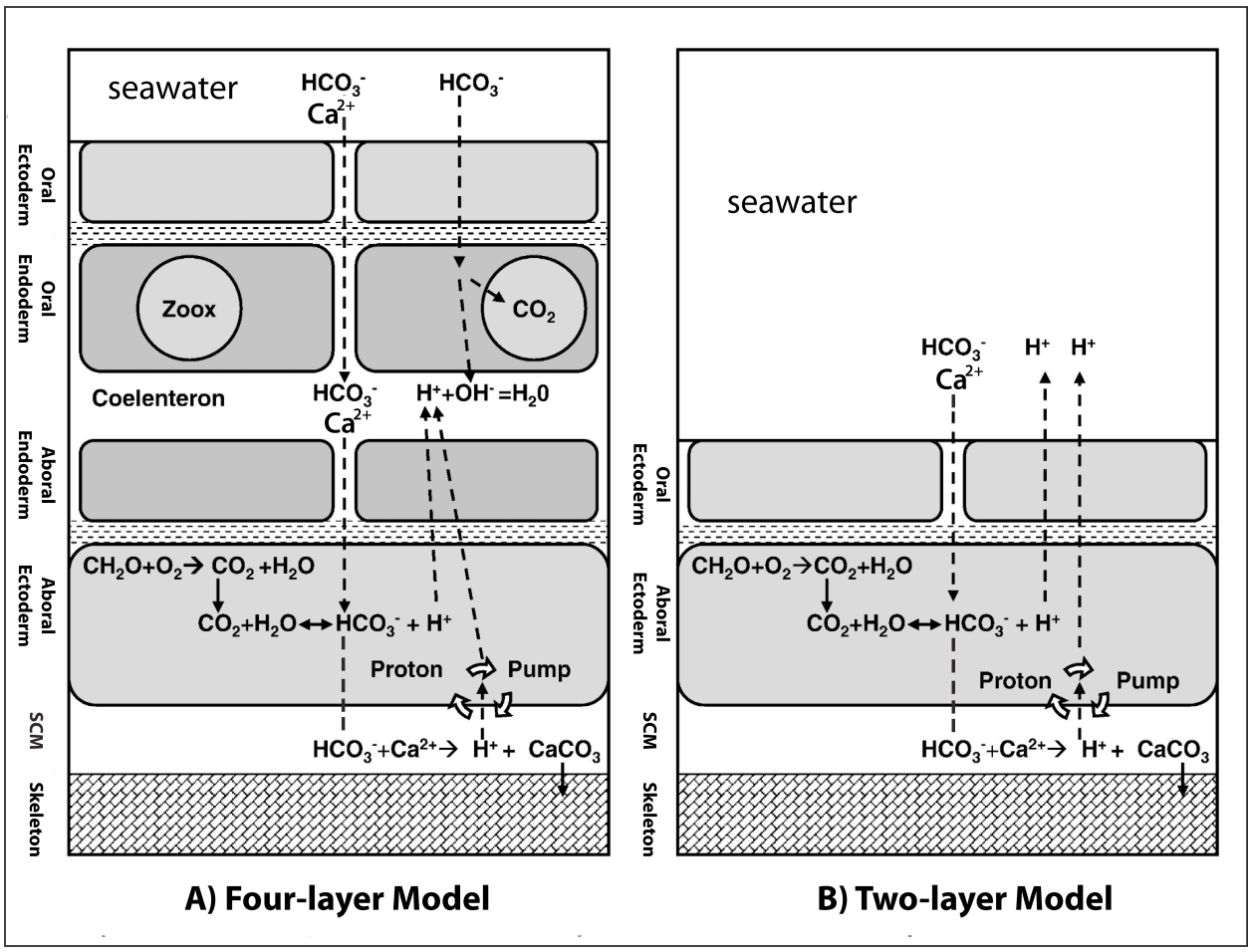

Figure 2. Coral Calcification Models. A) Traditional four-layer model for coral calcification showing potential pathways for transcellular and paracellular Ca^{2+} and HCO_3^- transport to the site of calcification in the subcalicoblastic medium (SCM). This model includes an unknown pump removing H^+ from the SCM. B) Two cell layer rapid calcification model containing only oral and aboral ectoderm (calicodermis) layers. Modified from Jokiel, (2011).

Another potential transcellular mechanism for Ca^{2+} transport is in vesicles, which are abundant in calicoblastic cells (Barrot et al., 2015a). In addition to Ca^{2+}, these vesicles could deliver the DIC and biomineralizing organic matrix proteins that are also needed for calcification (Tambutté et al., 1996). Supporting the role of vesicular transport in coral calcification, a recent study has shown the presence of ~400 nm amorphous calcium carbonate (ACC) particles in calicoblastic cells of *S.pistillata* (Mass et al., 2017). This proposed calcification mechanism involves uptake of seawater via vesicles in the oral ectoderm and transfer through coral tissue

layers to the calicoblastic cells, where biomineralization is initiated (Mass et al., 2017). The vesicles would then fuse to the apical membrane of the calicoblastic cells and their contents discharged into the SCM, where the precursors remain amorphous before final crystallization (Mass et al., 2017). However, it is not clear how vesicles may move through the oral ectoderm to the calicodermis. This potential mechanism has only been studied in one coral species, so further work is needed to confirm if it applies to other coral species. In any case, vesicular transport of ACC is not mutually exclusive with the mechanisms of ion-transport described above.

While Ca^{2+} for coral calcification comes exclusively from seawater, there are multiple potential sources of DIC. HCO_3 and CO_3^{2-} from seawater could be potentially transported to the SCM (Allison et al., 2014). Mitochondria, which are abundantly present in the calicoblastic cells, produce CO_2 by aerobic respiration that can be immediately hydrated into HCO_3^- and H^+ ions by carbonic anhydrase in the cell cytoplasm; the HCO_3^- may then be transported to the SCM. In fact, some studies reported that ~80% of the DIC used in calcification is of metabolic origin, although this cannot be generalized for all coral species (reviewed in Tresguerres et al., 2017). However, other studies have reported the respiration rate of coral is too low to be a single and consistent source of DIC for calcification (Falkowski et al., 1984), suggesting other DIC sources for skeleton formation.

Once Ca^{2+} and DIC combine into aragonite in the SCM, H^+ are produced as a byproduct of calcification (Figure 2). H^+ removal is essential to avoid SCM acidification that otherwise would decrease the aragonite saturation state and slow down calcification. The mechanisms for H^+ removal from the SCM into the calicoblastic cells are unknown. As previously stated, some studies hypothesize PMCAs; however, this would require PMCAs to be located in the apical membrane of calicoblastic cells, which does not seem to be the case (Barrot et al., 2015a). In

addition, H^+ must then be transported across the basolateral membrane of calicoblastic cells, into the mesoglea and aboral gastrodermal cells, then finally into the coelenteron.

One last constituent that has been identified in the coral skeleton and in the calicoblastic cells is the skeletal organic matrix (SOM), which is a collection of various proteins, lipids, and polysaccharides that is considered important "as a substrate, catalyst, or controlling agent in the chemical reactions that culminate in the deposition of new skeletal material" (Johnston, 1980). Some of the proteins found in the SOM are coral acid-rich proteins (CARPs) and a carbonic anhydrase enzyme. CARPs have the ability to catalyze the precipitation of $CaCO_3$ in vitro even at a pH of 7.6, a condition where crystallization would normally not take place (Mass et al., 2013). The carbonic anhydrase likely increases the rate of metabolic CO_2 hydration into HCO_3^-, which can then be used for calcification in the calicoblastic cells and the SCM (Moya et al., 2008).

Coral calcification rates increase in the presence of light, a phenomenon termed "light-enhanced calcification" (Chalker & Taylor, 1975). While the exact mechanisms behind light-enhanced calcification are still not completely understood, it is predicted that photosynthesis by *Symbiodinium* enhances calcification rates in multiple ways. It is possible that photosynthesis provides the carbohydrates needed as an energy source to fuel the energetically costly transport of DIC and maintenance of the alkaline pH of the SCM (Allemand et al., 2004). Photosynthesis could also provide the oxygen necessary for aerobic metabolism and the skeletal organic matrix precursors that assist in crystallization (Allemand et al., 2004). Additionally, photosynthesis could also be repurposing the waste products from calcification, such as CO_2, H^+, PO_4^{3-}, and NH_4^+ (Allemand et al., 2004).

The majority of a coral colony has four tissue layers, however, tissues at areas of rapid calcification, such as the tip of the coral branch in some species (Jokiel, 2011) and the skeletal spines (Tambutté et al., 2007) only have oral ectoderm and calicodermis, lacking gastrodermal tissues with symbiocytes. This is known as the two-cell layer model (Jokiel, 2011) (Figure 2B) and has important implications for coral calcification mechanisms since the lack of nearby *Symbiodinium* implies other mechanisms that deal with the H^+ produced by biomineralization. These zones of rapid calcification are prominent in some branching corals, including *Acropora* species, which are fast-growing and display a rapid development of structural complexity as they settle and grow (Guest et al., 2011).

Acid/Base Regulation

Metabolic activity produces H^+ (both directly and *via* CO_2 hydration) that acidify the intracellular environment (Fliegel & Fröhlich, 1993). Since a stable pH is essential for enzyme function and homeostasis, intracellular pH (pHi) must be tightly regulated (Madshus, 1988; Putnam & Roos, 1997). Cells regulate their pHi using two types of general mechanisms: (1) buffering and (2) active transport of H^+ and other acid/base equivalents. In addition, larger and more active animals maintain blood acid/base homeostasis by excreting and absorbing H^+ and HCO_3^- using specialized organs such as kidneys (Hamm et al., 2015) and gills (Evans et al., 2005), and by ventilatory adjustments that accumulate or get rid of CO_2.

Since corals do not have organs or blood, each coral cell must regulate pHi by buffering and by excreting and absorbing H^+ and HCO_3^- to and from seawater, the coelenteron, or the SCM, depending on the cell type. Knowledge about cnidarian buffering capacity is limited. The buffering capacity of gastrodermal cells from the anemone *Anemonia viridis* was reported to be

between 20.8 and 43.8 mM/pH unit, with cells containing *Symbiodinium* having slightly higher values than cells without *Symbiodinium* (Laurent et al., 2014). This study also reported *A. virdis* gastrodermal cells have a pHi recovery mechanism that is dependent on Na^+ and is sensitive to amiloride, a pharmacological inhibitor of solute carrier transporter 9 (SLC9) proteins (Laurent et al., 2014), which are proteins known to transport Na^+ and are involved in pH regulation (Donowitz et al., 2013), however further evidence for SLC9 proteins in *A. viridis* cells was not provided.

In addition, corals have the ability to generate and maintain extreme acidic pH levels in the symbiosome (pH~4), and alkaline pH levels in the SCM (pH~9). In the symbiosome space of symbiocytes, an acidic pH favors the speciation of DIC into carbon dioxide, making carbon more readily available for photosynthesis to occur. In *S. pistillata,* the pH is ~4 within the symbiosome space, while the pH in the cytoplasm of symbiocytes is ~7.10 (Barott et al., 2015b). This 1,000-fold difference in $[H^+]$ across a single membrane is possible because of vacuolar-H^+-ATPase (VHA) activity that transports H^+ across the symbiosome membrane into the symbiosome space (Barrot et al., 2015b).

The opposite scenario occurs in the SCM. The pH in the SCM ranges from 8.1 to 8.4 pH units at night and from 8.7 to 9.3 pH units during the day, with exact values dependent on the species and measurement methods used (Al-Horani et al., 2003; A. Venn et al., 2011). However, the cytoplasm of the calicoblastic cells is ~7.4 pH units in both light and dark conditions, identifying another region where coral maintains stark differences in pH separated by a single membrane (Venn et al., 2011).

Recent advances in coral transcriptomics and genome analysis (Sea-quence project: ReFuGe 2020 Consortium) allows for the identification of coral gene products and prediction of

their physiological roles based on homologous proteins with known functions in better studied organisms. SLC9 proteins (*SLC9* family, Cation proton antiporter (*CPA*) superfamily) are a class of proteins involved in pH regulation in all organisms studied so far that are likely to also play important roles in corals. To my knowledge, the only relevant study on cnidarians found that amiloride, a pharmacological inhibitor of mammalian SLC9 proteins, impaired pHi regulation in *A. viridis*, speculating the presence and functional importance of SLC9 proteins in this mechanism (Laurent et al., 2014). However, that study did not clone the potential *SLC9* gene(s), identify the protein, or characterize where it was expressed. Abundant information is available for SLC9s from model species, especially mammals.

SLC9 Proteins

SLC9s are a family of proteins that transport Na^+ into cells and H^+ out of cells in a 1:1 ratio (Xu et al., 2018), and are used by almost all eukaryotic cells to regulate pHi (Fliegel & Fröhlich, 1993). The *SLC9* gene family includes 3 subfamilies: *SLC9A, SLC9B*, and *SLC9C*. *SLC9A* codes for the Na^+/ H^+ exchangers (NHE1-9 in mammalian systems) and belongs to the *CPA1* superfamily; the SLC9B subfamily belongs to the *CPA2* superfamily and codes for the Na^+/ H^+ antiporters (NHAs). The *SLC9C* subfamily is categorized into the Na^+-transporting carboxylic acid decarboxylase *(NaT-DC*) superfamily and codes for sperm-specific NHEs and a SLC9C2 protein, referred to as NHE 11 in human systems. There is some debate as to whether this subfamily belongs within the *SLC9* family because it does not show a strong homology with the mammalian NHEs and NHAs and is only weakly related to the other *NaT-DC* members, (Brett et al., 2005) (Figure 3).

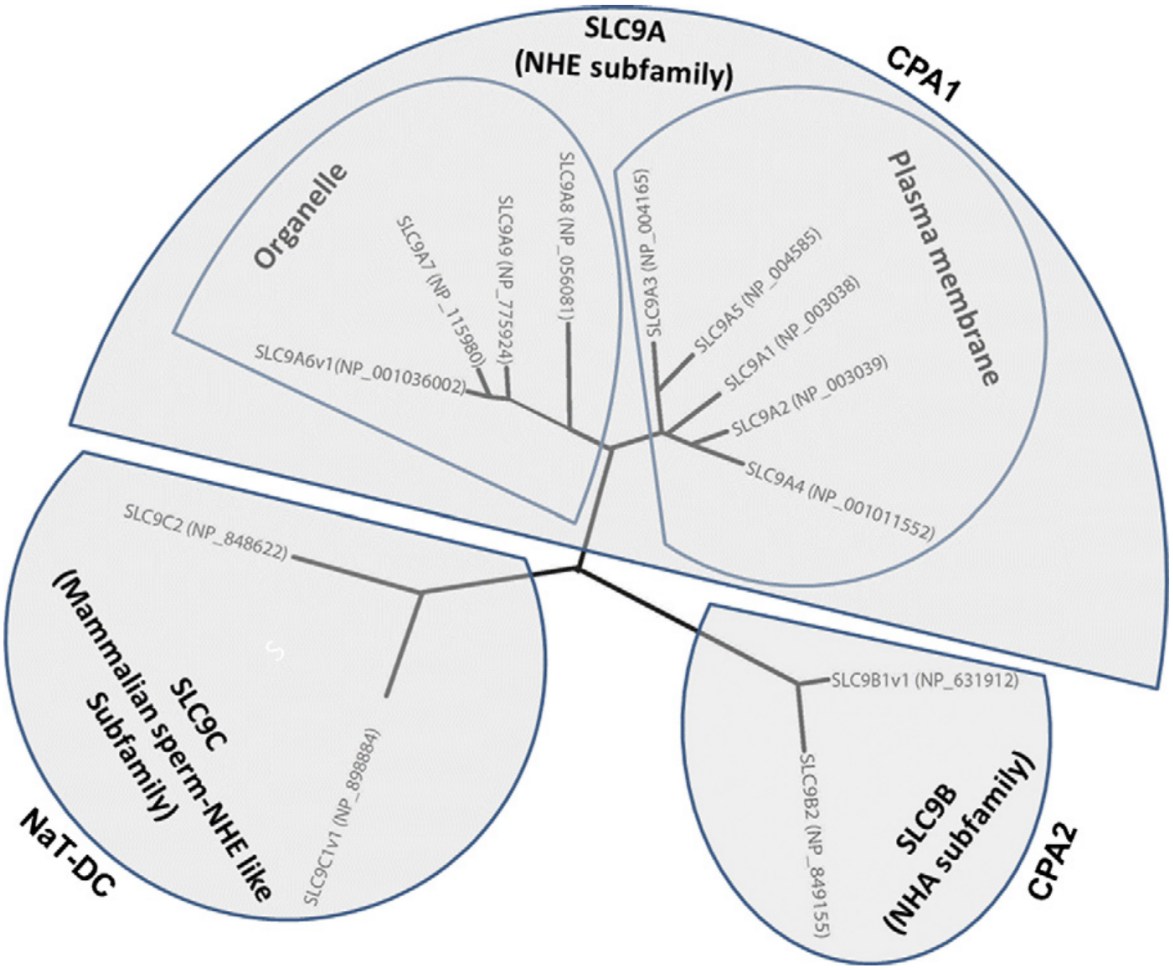

Figure 3. NHE Family Phylogenetic Tree. NHE proteins are grouped into three subfamilies: *SLC9A*, *SLC9*B and *SLC9C*. The *CPA1/SLC9A* is further classified into organelle and plasma membrane NHEs. From Donowitz et al (2013).

Despite the high diversity of SLC9 proteins, they all share certain features. All SLC9 proteins have two regions, an N-terminus region with 10-12 transmembrane domains where the exchange of the Na^+ and H^+ occurs, and a polar, intracellular C-terminus that varies in length and is involved in the regulation of the protein activity (Fliegel & Fröhlich, 1993; Donowitz et al., 2013). The C-terminus interacts with intracellular regions of the N-terminus, as well as with negatively charged phospholipids on the internal side of the plasma membrane (Alexander et al., 2011; Ikeda et al., 1997). Bioinformatic analyses using fold alignment algorithms combined with

mutagenesis studies of mammalian NHE1 and the bacterial NHA1 predicted a two-inverted funnel area in the center of the N-terminus where the exchange of the Na^+ and H^+ ions takes place (Donowitz et al., 2013). This structure also contains a pH sensor domain that plays a role in proton movement regulation, but is separate from the ion-exchanging transport funnel and a dimerization domain (Donowitz et al., 2013). The funnel transport region is present in at least twelve other gene families and is a potential general transport mechanism (Hu et al., 2011). While SLC9 monomers are sufficient for Na^+/ H^+ transporting activity, all SLC9 proteins form dimers within the membrane that are believed to provide structural support (Fliegel & Fröhlich, 1993; Donowitz et al., 2013). SLC9 proteins are also known to undergo post-translational modifications such as glycosylation and phosphorylation, which affect activation, regulation, trafficking, transport, and increases SLC9 protein size (Fliegel & Fröhlich, 1993; Donowitz et al., 2013). Specific types and locations of glycosylation and phosphorylation are different between each of the SLC9 protein members and details are still unknown in some of the less studied SLC9 proteins.

Na^+/H^+ exchange is driven by the inside directed [Na^+] gradient generated by the Na^+/K^+-ATPase (NKA), which uses energy made available by the removal of a phosphate group bonded to adenosine-triphosphate (ATP), to keep intracellular [Na^+] at much lower levels compared to extracellular fluids (Figure 4A). This allows for the secretion of H^+ in exchange for Na^+, even against a [H^+] gradient (Fliegel & Fröhlich, 1993). They are often involved in regulating pHi and also play roles in cell volume regulation and osmoregulation (Xu et al., 2018). Some SLC9 proteins are present in intracellular locations such as endosomal vesicles (Donowitz et al., 2013) (Figure 4B), the Golgi apparatus, (Nakamura et al., 2005), and the endoplasmic reticulum (Miyazaki et al., 2001), where they maintain specific pH necessary for specific physiological

function, such as digestion, protein modification, and trafficking. A large number of SLC9 proteins are found in intestinal, digestive, and gill epithelia, where they are involved in Na^+ absorption (Figure 4C). Often, multiple isoforms of SLC9 proteins are found within the same tissues and are involved in the same physiological process, such Na^+ uptake, but localize to different membranes.

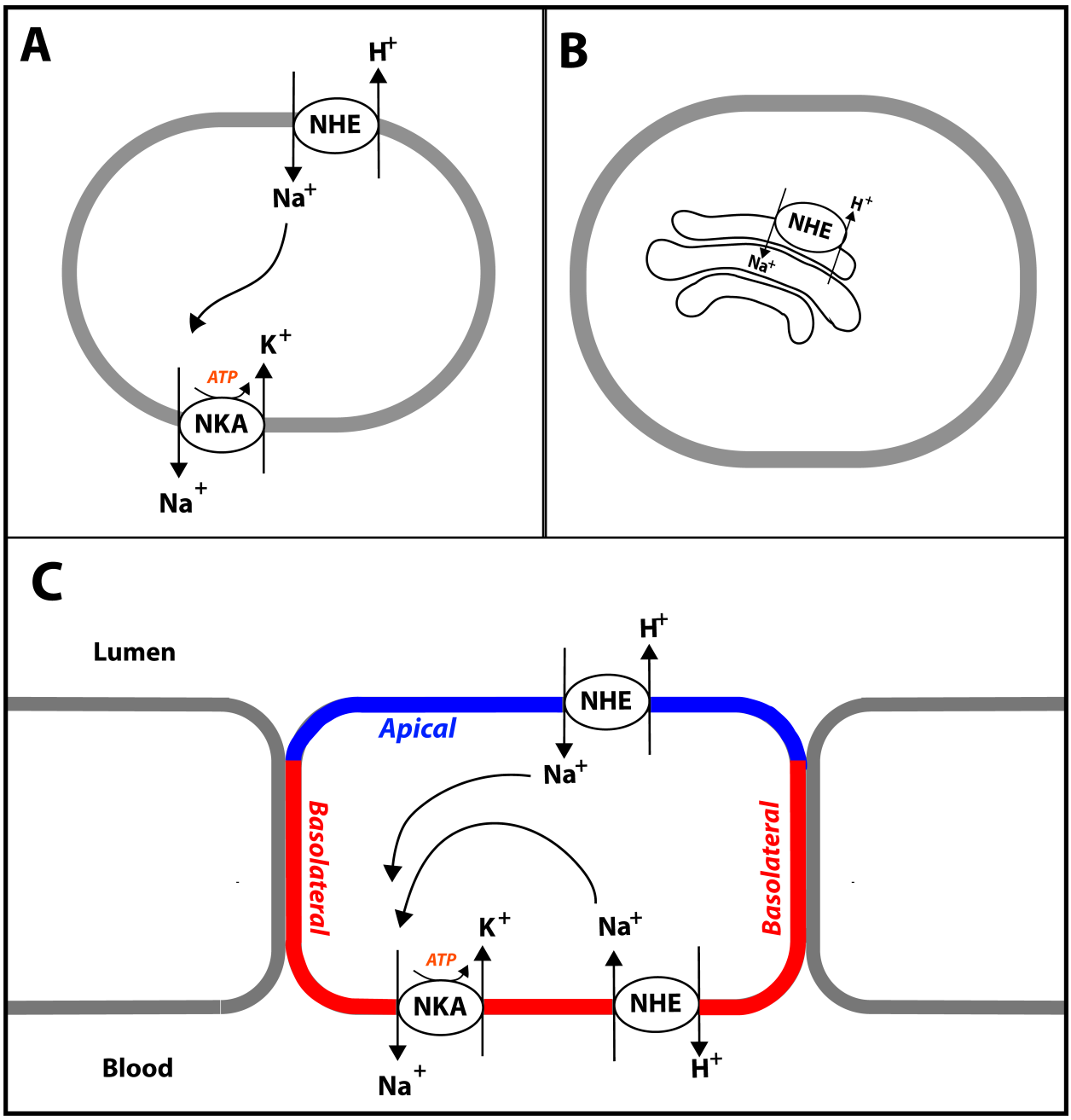

Figure 4. Potential SLC9A subcellular localizations. A) SLC9A proteins (Na^+/H^+ Exchangers (NHE) 1-9) are driven by Na^+/K^+-ATPase (NKA) secondary active transport in a non-polarized cell. B) NHEs in intracellular organelle. The Golgi apparatus is shown here, but NHEs are also present in the Endoplasmic Reticulum, endosomes, and lysosomes. C). NHE driving by NKA activity in a polarized cell. Some NHE isoforms are present in the apical membrane and secrete H^+ and absorb Na^+, while others are present in the basolateral membrane and absorb H^+.

SLC9A Subfamily (NHEs)

The *SLC9A* subfamily belongs to the *CPA1* subgroup of the *CPA* superfamily, are commonly referred to as NHEs, and has 9 members (NHE1-9). NHE1 is well characterized, and is present in the plasma membrane of most mammalian cells (Donowitz et al., 2013). In polarized cells, NHE1 localizes to the basolateral membrane, yet in non-polarized migratory fibroblasts, NHE1 localizes to the leading edge of the cell near the lamellipoda (Donowitz et al., 2013). NHE1 undergoes both N- and O- glycosylation, but neither are required for activation or transport. NHE1 is regulated by ubiquitination, the inactivation of a protein by the attachment of a ubiquitin molecule (Simonin & Fuster, 2010). The main role of NHE1 is preventing pHi acidification, but at least in mammalian cells, it also precipitates a cell volume restoration mechanism through the transport of Na^+ into the cell that is coupled with the uptake of Cl^- and H_2O (Donowitz et al., 2013). NHE1 potentially has other functions since it has been found in other cellular locations, such as intercalated disks and T-tubules in cardiac myocytes, however, those alternative localizations are infrequent, and the functions are not known.

NHE2 is found in epithelial cells. In stomach cells, the brush border of the colon, gallbladder, and small intestine, it is present in the basolateral membrane (Donowitz et al., 2013). However, in renal cells, the ascending limb of Henle, and the distal convoluted tubules within the kidney of mammals, NHE 2 is in the apical membrane (Donowitz et al., 2013). The physiological role of NHE2 has not been completely elucidated, but there is evidence that it is involved in intestinal and renal Na^+ absorption. However, the extent of NHE2 involvement in intestinal Na^+ absorption is organism specific, and NHE2 activity is often supplemented by NHE3 (Donowitz et al., 2013). In the colon, NHE2 is linked to a short-chain fatty acid/HCO_3^- exchanger (Subramanya et al., 2007), providing interesting implications when studying DIC

transport for calcification in corals since the transport of HCO_3^- and H^+ in opposite directions is necessary along the border of the calicoblastic cells and the SCM. NHE2 is also potentially involved in epithelial damage repair mechanisms (Donowitz et al., 2013; Xue et al., 2011). NHE2 appears to have only O-linked glycosylation (Orlowski & Grinstein, 1997; Tse et al., 1994).

NHE3 is abundantly expressed in a large variety of mammalian tissue and cell types and its localization to the apical or basolateral membrane is highly species-specific. It is found in the small intestine, colon, gallbladder, renal proximal tubule, thick and thin limbs of the loop of Henle, gastric parietal cells, epididymus, ovary, thymus, prostate, some respiratory neurons in the ventrolateral medulla oblongata, and in the rostral extension of the retrotrapezoid nucleus/parapyramidal region in the pons (Hoogerwerf et al., 1996). NHE3 is responsible for the majority of renal and intestinal Na^+ absorption, as well as for glucose uptake and whole body volume homeostasis in the kidneys (Donowitz et al., 2013). NHE3 is consistently trafficked between intracellular vesicles and the cell plasma membrane; it is one of the most regulated transport proteins on acute and long-term scales (Donowitz & Li, 2007; Donowitz et al., 2013). NHE3 glycosylation is essential for trafficking to the cell plasma membrane (Soleimani et al., 1996). Potentially relevant for coral symbiosomes, NHE3 interacts with VHA to acidify organelles involved in cellular recycling pathways; however, the details of this interaction are not known (Donowitz et al., 2013).

In humans, NHE4 is most abundantly expressed in the stomach, and at lower levels in the kidney medulla, hippocampus, zymogen granule of pancreas, and salivary gland (Donowitz et al., 2013). NHE4 is generally localized to the basolateral membrane of those epithelial cells and is often found together with NHE1 (Donowitz et al., 2013). The functional roles of NHE4 are not

well known. One of its few established roles is in NH_4^+/NH_3 absorption in conjunction with the apical $Na^+/K^+/2Cl^-$ cotransporter (NKCC) (Donowitz et al., 2013; Eladari & Chambrey, 2010). Studies on mouse cell lines suggested a potential function in volume regulation in parietal cells, together with anion exchanger 2 (Bourgeois et al., 2010; Donowitz et al., 2013; Gawenis et al., 2005). It seems that NHE4 is not involved in pHi regulation, which is unusual for a NHE (Bourgeois et al., 2010; Donowitz et al., 2013; Gawenis et al., 2005).

The expression of human NHE5 is much more specific than the other NHEs, being exclusively present in sperm and neurons (Donowitz et al., 2013). While the presence of NHE5 in sperm has been confirmed by Western blotting, its function has not been determined (Woo et al., 2002). In neurons, it was recently elucidated that NHE5 is involved in regulating the pH of the synaptic cleft (Donowitz et al., 2013). The acidification of this region may serve as an autocrine feedback mechanism that regulates post-synaptic receptors, and as a paracrine mechanism that regulates pre-synaptic proteins such as voltage-gated Cl^- channels that are important in neuron signaling and synaptic firing (Diering et al, 2011). NHE5 shares strong (~50%) amino acid identity with NHE3, suggesting similar physiological functions and regulatory properties (Donowitz et al., 2013). NHE5 can be found in both the cell plasma membrane and in recycling endosomes. Trafficking and activation at these two locations is reliant on a multitude of enzymes. In particular, phosphorylation is required for internalization of NHE5 in recycling endosomes (Donowitz et al., 2013).

In mammalian systems, NHE6, NHE7, and NHE9 localize to various organelles and are, therefore, categorized as "intracellular NHEs" (Donowitz et al., 2013). Each of these NHEs is believed to be related to the NHX1 protein in *S. cerveciae*, which serves as a model protein for the physiological function and regulation for these three NHEs (Donowitz et al., 2013). While

other NHEs in the SLC9A family exchange Na^+ ions with H^+ ions, NHE6, 7, and 9 are Na^+ and K^+/H^+ exchangers, showing similar Vmax and Km for Na^+ and K^+ (Donowitz et al., 2013). The general function of these NHEs is to regulate intraorganellular pH, as demonstrated by an increase in intraorganellular pH induced by overexpression of these NHEs (Donowitz et al., 2013; Nakamura et al., 2005). NHE6 is present in recycling endosomes (Brett et al., 2002); NHE7 is in the trans-Golgi (Numata & Orlowski, 2001; Orlowski & Grinstein, 1997); and NHE9 is in recycling endosomes, late endosomes and lysosomes (Nakamura et al., 2005). NHE6 can sometimes present at very low levels in the plasma membrane, and NHE7 has been shown to also traffic to recycling endosomes and the plasma membrane (Donowitz et al., 2013).

NHE8 has alternatively been described to localize to both the plasma membrane and intracellular organelles. It shares about 25% homology with the other NHEs and its C-terminus is 5-100 amino acids shorter than others in the family, sharing no amino acid similarity. This implies that NHE8 is differentially regulated compared with the other NHE family members. In mosquito Malpighian tubules, NHE8 is intracellularly located, and in mammalian cells it is localized to the mid- and trans-Golgi, and, at a lesser extent, in endosomes (Kang'ethe et al., 2007; Nakamura et al., 2005). NHE8 is also found to localize apically in renal proximal tubules and in the intestine (Donowitz et al., 2013). Intracellular NHE8 is believed to be involved in endosomal pH control, which has further effects on driving and controlling processes such as protein trafficking and inward vesicularization (Donowitz et al., 2013). While NHE3 is believed to be the main brush border NHE in adults that is involved in intestinal tract Na^+ absorption, it is believed that NHE8 is the main renal and intestinal brush border NHE in neonates (and still contributing at minor levels in adults) (Becker et al., 2007; Xu et al., 2018).

SLC9B Subfamily (NHAs)

The *SLC9B* subfamily belongs to the *CPA2* subgroup of the *CPA* superfamily and characterizes a group of eukaryotic NHAs more closely related to prokaryotic NHAs, such as *E. coli* NhaA. Therefore, the two proteins in this subfamily are termed NHA1 and NHA2 (Donowitz et al., 2013). NHAs have 12 transmembrane domains and differ from other SLC9 proteins by having a much shorter N- and C-terminus (Donowitz et al., 2013). NHA1 is expressed in testis, in the apical membrane of Malphigian tubules in *Drosophila melanogaster*, and in the plasma membrane of *S. cerevisaie* (Donowitz et al., 2013). However, the physiological functions of NHA1 remain unclear. NHA2 was originally discovered through knockout and upregulation studies in osteoclast cells (Battaglino et al., 2008), and subsequently discovered in mouse tissues including brain, heart, lung, liver, kidney, pancreas, spleen, stomach and colon (Fuster et al., 2008; Xiang et al., 2007). NHA2 can be present in the plasma membrane as well as intracellularly. Evidence from yeast expression studies, chromosomal localization, transport properties, regulatory characteristics, and other localization evidence have led researchers to believe that NHA2 is a Na^+/Li^+ cotransporter (Xiang et al., 2007). It has also been found in a renal tubular segment of rat kidney that is known to be important in organismal Na^+ absorption and homeostasis maintenance (Donowitz et al., 2013; Fuster et al., 2008). Overall, specifics on localization are still fairly unknown for the two isoforms within this subfamily.

SLC9C Subfamily

Finally, the *SLC9C* subfamily belongs to the *NaT-DC* superfamily and contains the sperm-specific NHEs. They were first identified in mouse spermatoid cDNA enriched libraries

(Wang et al., 2003; 2007). These SLC9s have an NHE-like N-terminus and a long, non-conserved, C-terminus that contains high similarity to *NaT-DC* members (Donowitz et al., 2013). Due to these differences, sperm NHEs were categorized as their own subfamily apart from *SLC9A* and *SLC9B* (Donowitz et al., 2013). These proteins are predicted to have 14 transmembrane domains and have two unique domains, a sensing motif and a cyclic nucleotide-binding domain (Wang et al., 2003). SLC9C knockout mice are completely infertile (Wang et al., 2003). The SLC9C2, known as NHE11 in mammalian systems, also belongs to this subfamily, but no functional data is available (Donowitz et al., 2013).

Thesis Purpose

The purpose of this thesis is to identify and characterize an SLC9 protein in the Scleractinian, complex coral, *Acropora yongei.* SLC9 proteins are involved in pH regulation in all other organisms studied, however, have yet to be identified in corals. Corals experience extreme acid/base disturbances as a result of essential physiological processes, such as photosynthesis and calcification, therefore, I hypothesize that SLC9 proteins are also likely important for coral cellular biology. Elucidating the role(s) of SLC9 proteins in coral cells first requires determining the presence of *SLC9* genes and their encoded proteins, and then characterizing its localization in different coral cell types. I performed bioinformatic analyses to identify genes coding for an SLC9-like protein in corals. I performed phylogenetic analysis, which further characterized this coral SLC9-like protein as an SLC9A, or NHE protein, and validated novel antibodies against it. Immunofluorescence analyses revealed that the *Acropora*NHE protein is abundantly expressed in calicoblastic cells, suggesting a physiological role in calcification.

MATERIALS AND METHODS

Coral culture

Colonies of *A. yongei* were obtained from the Birch Aquarium at Scripps, in La Jolla, CA and maintained in a flow-through seawater tank system at 25°C on a 10hr/14hr hour light: dark cycle with dawn and dusk light preceding sunrise (08:00) and sunset (18:00) by 15 minutes. Stimulated moonlight followed the dusk lighting for 4 hours at the beginning of the 14-hour dark period. These settings are provided by Orbit Marine LED Fixture model 4103-B lights with the M3 lighting program. Tanks were cleaned twice a week to clear algal growth on aquaria and coral stands and specimens were allowed to acclimate for at least 3 days prior to sampling.

Antibody Development

An NHE-like sequence (GenBank: JT000139.1) was identified from the *A. millepora* genome via BLAST search using human NHE1 (SLC9A1; UniProtKB/Swiss-Prot: P19634.2) as the query sequence. Another NHE-like sequence (adi_EST_assem_7750) was identified from the *A. digitifera* genome via BLAST search using *A.millepora* NHE as the query sequence. Custom rabbit polyclonal anti-NHE antibodies (initially termed NHE_A, NHE_B, NHE_C) were developed against three epitope regions present in the NHE sequences from both *Acropora* species (Genscript USA, Inc.). The epitope regions are as follows: NHE_A: EEDVEPNKGKPARP; NHE_B: ETDGGDQNRKSSPT; NHE_C: REGSGAALFKNSTE. Antibody specificity was tested for Western Blotting and immunofluorescence as described below. Based on those results, anti-*Acropora*NHE_B was used for subsequent characterization of NHE in *A. yongei* tissues. These antibodies are referred to as "anti-*Acropora*NHE antibodies".

Sequence phylogenetic and post-translational analysis

Sequences for phylogenetic analysis were found by BLAST search using the NCBI protein database. Sequences were then formatted and uploaded into phylogeny.fr. Here they were aligned using MUSCLE, curated by Gblocks, and a tree rendered with a 500 bootstrap comparison and re-rooted against *S. salivarius* NHA, a prokaryotic Na^+/H^+ antiporter (Dereeper et al., 2010). Visualization modifications were made in FigTree (v1.4.3). The *A.millepora* and *A.digitifera* NHE sequences were then analyzed for post-translational modifications, specifically glycosylation and phosphorylation. Glycosylation sites were predicted using The Hirst Group Glycosylation Predictor (http://comp.chem.nottingham.ac.uk/glyco/, Hamby & Hirst, 2008), and compared to known glycosylation in human NHE1, rat NHE1, and rat NHE2 reported in Fliegel and Fröhlich (1993). The two coral sequences and three mammalian NHEs were aligned using MUSCLE, and the image was generated using Geneious version 8.1 (http://www.geneious.com, Kearse et al., 2012). Transmembrane domains were predicted using the DTU Bioinformatics TMHMM (Server v. 2.0). N- and O-glycosylation sites were predicted using the DTU Bioinformatics NetNGlyc 1.0 Server (http://www.cbs.dtu.dk/services/NetNGlyc/, Gupta et al., 2004) and NetOGlyc 4.0 Server (http://www.cbs.dtu.dk/services/NetOGlyc/, Steentoft et al, 2013). Phosphorylation sites were predicted using the DTU Bioinformatics NetPhos 3.1 Server (http://www.cbs.dtu.dk/services/NetPhos/, Blom et al., 2004). The rendered 3D folded structure was generated using the intensive mode setting on Phyre2 web portal for protein modeling, prediction and analysis (http://www.sbg.bio.ic.ac.uk/phyre2/html/page.cgi?id=index, Kelly et al., 2015).

Antibody Verification via Western Blotting

Coral fragments were processed for Western blotting following the protocols described in Barott et al. (2015a), with some modifications. Tissue was homogenized using a pressurized airbrush in S22 buffer (450 mM NaCl, 10 mM KCl, 58 mM $MgCl_2$, 10 mM $CaCl_2$, 100mM Hepes, pH 7.8) with 1mM dithiothreitol(DTT), 1mM phenylmethylsulfonyl fluoride(PMSF) and 10mM benzamidine hydrochloride hydrate (BHH). *Symbiodinium* were pelleted from the homogenate by centrifugation at 500 rcf for 15 minutes in 4°C. Aliquots of the supernatant were taken and labeled crude homogenate. The tissue was further fractionated by centrifugation at 3220 rcf for 30 minutes in 4°C; the supernatant was enriched for soluble proteins and the pellet was enriched in membrane proteins (Figure 5). The pellet was then resuspended in ~150 µL of homogenization buffer. Protein concentration was determined in all fractions using the Bradford Assay with a bovine serum albinum (BSA) standard curve (standards of 0.9 µg- μL^{-1}, 0.7 µg- μL^{-1}, 0.56 µg- μL^{-1}, 0.28 µg- μL^{-1} and 0.14 µg- μL^{-1}).

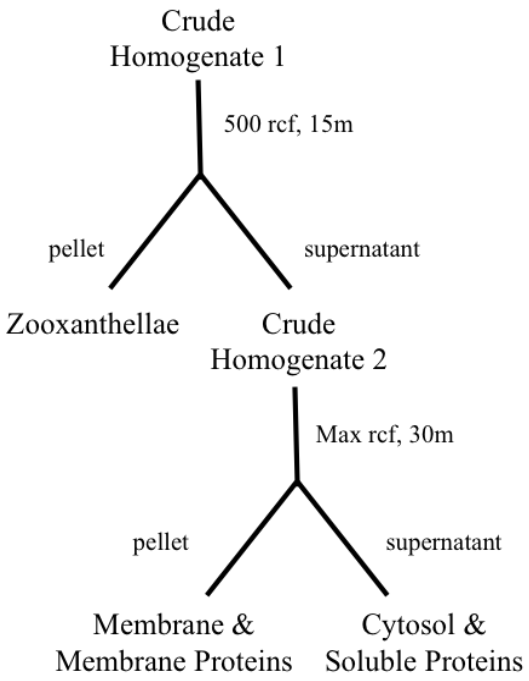

Figure 5. Summary of coral tissue fractionation by centrifugation used to enrich for membrane proteins, such as NHE. From Perez, Master's thesis.

Tissue homogenates were then incubated in Laemmli Sample Buffer containing 5% (vol/vol) β-mercaptoethanol for 15 min at 70°C and loaded into a 1.5 mm-10 lane SDS-PAGE gel. Following separation, proteins were transferred to a PVDF membrane by the overnight BioRad wet transfer system, utilizing Towbin Buffer (25 mM Tris, 192 mM glycine, 20% (vol/vol) methanol, pH 8.1-8.5). The next day, the membrane was incubated in blocking buffer (Tris-buffered saline and 0.1% Tween detergent (TBS-T) + 5% fat-free milk) for 1 hr at room temperature and then incubated overnight at 4°C with anti-*Acropora*NHE antibodies (0.3 μg-mL^{-1}) on an orbital shaker. The membrane was then washed three times in TBS-T for 15 min each, incubated with secondary antibodies (goat anti-rabbit HRP; diluted in blocking buffer at 1:10,000), and washed three more times in TBS-T for 15 min each. Bands were visualized with a 1:1 solution from the enhanced chemi-luminescence kit and imaged with a BioRad Chemidoc

Imaging System. Samples were run along with a BioRad Precision Plus Protein Pre-stained Standards Dual Color to determine relative protein molecular weight.

Preabsorption peptide controls were performed to further validate the anti-*Acropora*NHE antibodies. A stock of anti-*Acropora*NHE_B was made in blocking buffer (0.3 μg- mL^{-1}) and split into two aliquots; the NHE_B antigen peptide was added to one of the aliquots at 400 fold excess in a molar basis (1.2 μg- mL^{-1}). Both aliquots were incubated overnight at 4°C and the peptide preabsorption control was added to a PVDF membrane containing replicate coral samples and processed for Western blotting as described above.

Deglycosylation

Coral tissues were processed as described above to obtain a fraction enriched in membrane proteins. Samples with and without the deglycosylation enzymes were processed following the Non-denaturing Reaction Conditions Protocol for Protein Deglycosylation Mix II developed by New England BioLabs Inc. Additional control samples were frozen at -80°C and then denatured in Laemmli Sample Buffer with 5% (vol/vol) β-mercaptoethanol for 15 min at 70°C and analyzed by Western-blotting as described above.

NHE Immunolocalization

Coral fragments were processed for immunofluorescence following the protocols described in Barrott et al. (2015a). Coral fragments were fixed overnight in S22 Buffer with 3% paraformaldehyde at 4°C and then decalcified in Ca^{+}-free S22 Buffer (450 mM NaCl, 10 mM KCl, 58 mM $MgCl_2$, 0.5 M EDTA pH 7.8) with 0.5% paraformaldehyde at 4°C. The buffer was

replaced daily until the skeleton was completely dissolved (~14 days). Tissues were then incubated in 50% ethanol for ~6 hours, transferred to 70% ethanol, and stored at 4°C. Tissues were dehydrated by incubation in 95% ethanol, followed by three consecutive incubations in 100% ethanol and three consecutive incubations in SafeClear (20 min each). Then, tissues were embedded in liquid paraffin (~40°C) for three consecutive incubations (30 min each). After hardening, the paraffin blocks were sectioned at 7, 8 and 10 μm using a rotary microtome. Sections were floated on a drop of water on glass slides and incubated on a hot plate for ~30 sec at ~36°C. The slides were left on a paper towel on the hot plate at ~30°C overnight in order for the section to adhere to the glass.

Tissue sections were then rehydrated by three consecutive incubations in SafeClear and one incubation in each 100% ethanol, 95% ethanol and 70% ethanol (10 min each). Tissue sections were then permeabilized in 1x PBS + 0.2% Triton-X detergent (PBS-T) for 10 min. Sections were blocked for 1 hr at room temperature with PBS-T containing 2% normal goat serum and 0.02% keyhole limpet hemocyanin, and subsequently incubated with the anti-*Acropora*NHE_B antibodies (3 μg- mL^{-1}) overnight at 4°C. Sections were washed three times in PBS-T for 5 min each, incubated with secondary antibodies (goat anti-rabbit Alexa555; diluted in blocking buffer at 1:500 dilution) and stained with Hoescht to visualize DNA (1:1000 in blocking buffer). Cover slips were mounted with Fluoro-gel containing Tris-Buffer (Electron Microscopy Sciences) and sealed with nail polish.

Controls were treated as above except no primary antibody was applied. Preabsorption peptide controls were performed to further validate the anti-*Acropora*NHE antibodies. A stock of anti-*Acropora*NHE_B was made in blocking buffer (3 μg- mL^{-1}) and split into two aliquots; the NHE_B antigen peptide was added to one of these aliquots at 400 fold excess in a molar basis (12

μg- mL^{-1}). The two antibody solutions were added to consecutive sections on the same slide and processed as described above.

The tip and base of four separate branches (N=4) were processed and analyzed. Immunofluorescence was detected using an epifluorescence microscope (Zeiss AxioObserver Z1) connected to a metal halide lamp and appropriate filters. Some images were captured using structured illumination (Zeiss Apotome 2). Digital images were adjusted for brightness and contrast only, using Zeiss Axiovision software and Image J software.

RESULTS AND DISCUSSION

Coral NHE Molecular Characterization

To my knowledge, this is the first identification and characterization of a NHE protein in corals. The *A.millepora* sequence has a conserved Na^+/H^+ exchanger domain from the *CPA1* superfamily. Further BLAST searches identified similar proteins in *A. digitifera, S. pistillata,* and *Orbicella faveolata*. Phylogenetic analysis revealed that these coral SLC9 proteins grouped together and are most closely related to the ancestral protein that gave origin to the mammalian NHEs 1-5 in the SLC9A subfamily (*CPA1* superfamily) (Figure 6), which are typically found in the cell plasma membrane. Other nucleotide sequences identified in *S. pistillata* and *O. faveolata* were more closely related to the mammalian intracellular NHEs 6-9 (also in the SLC9A subfamily), or to mammalian SLC9Bs (*CPA2* superfamily).

I focused on the *Acropora* SLC9 protein most closely related to mammalian NHE1-5, which is referred to as "*Acropora*NHE" in this thesis. Topology analysis predicts *Acropora*NHE has 10 transmembrane domains (Figure 7A), which is within the typical 10-12 transmembrane

domains of the NHE family (Donowitz et al., 2013). The end of the sequence contains a long, extended structure (amino acid 352-728) that is predicted to be outside of the cell (predicted to be amino acids 352-728 of *A. millepora* NHE) (Figure 7A). This structure could be a large C-terminus domain, which is characteristic of all eukaryotic NHEs (Nakamura et al., 2005). A 3D model showing the predicted folding structure of *Acropora*NHE with ~89% of the residues modeled at >90% confidence is shown in Figure 7B.

Figure 6. NHE Phylogenetic Tree. Phylogenetic tree of NHE isoforms in the three subfamilies. *A.millepora* NHE and *A.digitifera* NHE are in blue and mammalian NHEs are in red. **Human (*Homo sapiens*)** NHE1 NP_003038.2; NHE2 AAI36378.1; NHE3 AAI43329.1; NHE4 Q6AI14.2; NHE5 Q14940.2; NHE6 Q92581.2; NHE 7 Q8BLV3.1; NHE8 XP_011527038.1; NHE9 NP_775924.1; SLC9B1 NP_631912; SLC9B2 NP_849155; SLC9C1 NP_898884; SLC9C2 NP_848622; **Mouse (*Mus musculus*)** NHE1 Q61165.1; NHE2 AAI04738.1; NHE3 G3X939.1; NHE4 Q8BUE1.1; NHE5 AAI51198.1; NHE6 AAI30222.1; NHE7 Q8BLV3.1; NHE8 Q8R4D1.1; NHE9 NP_808577.3; SLC9C Q6UJY2.3; **Salamander (*Amphiuma tridactylum*)** NHE1 AAD33928.2; **Yellowtail (*Seriola lalandi dorsalis*)** XP_023257580; **Zebrafish (*Danio rerio*)** NHE 1 ABU68832.1; NHE 2 NP_001107567.1; NHE 3 XP_021323799.1; NHE 5 ABU68835.1; NHE6 ABU68836.1; NHE7 NP_001025248.2; NHE8 AAI65875.1; **Fruitfly (*Drosophila melanogaster*)** NHE1 AAF51559.3; NHE2 NP_001137851.1; NHE3 AAF13702.1; **Roundworm (*Caenorhabditis elegans*)** NHX AAM18109.1; NHX2 Q8T5S1.1; NHX3 O16452.2; NHX7 G5EBK1.1; ***Stylophora* Coral (*Stylophora pistillata*)** NHE1 XP_022782759.1; NHE2 PFX30385.1; NHE9 XP_022801109.1; NHE9 PFX18952.1; NHE10 XP_022780041.1; NHE10 PFX32044.1; ***Orbicella* Coral (*Orbicella faveolata*)** NHEbeta-like XP_020603608.1; NHE6 XP_020605233.1; NHE10 XP_020617264.1; **Sea anemone (*Exaiptasia pallida*)** NHE XP_020905858.1; NHE3 KXJ11245.1.

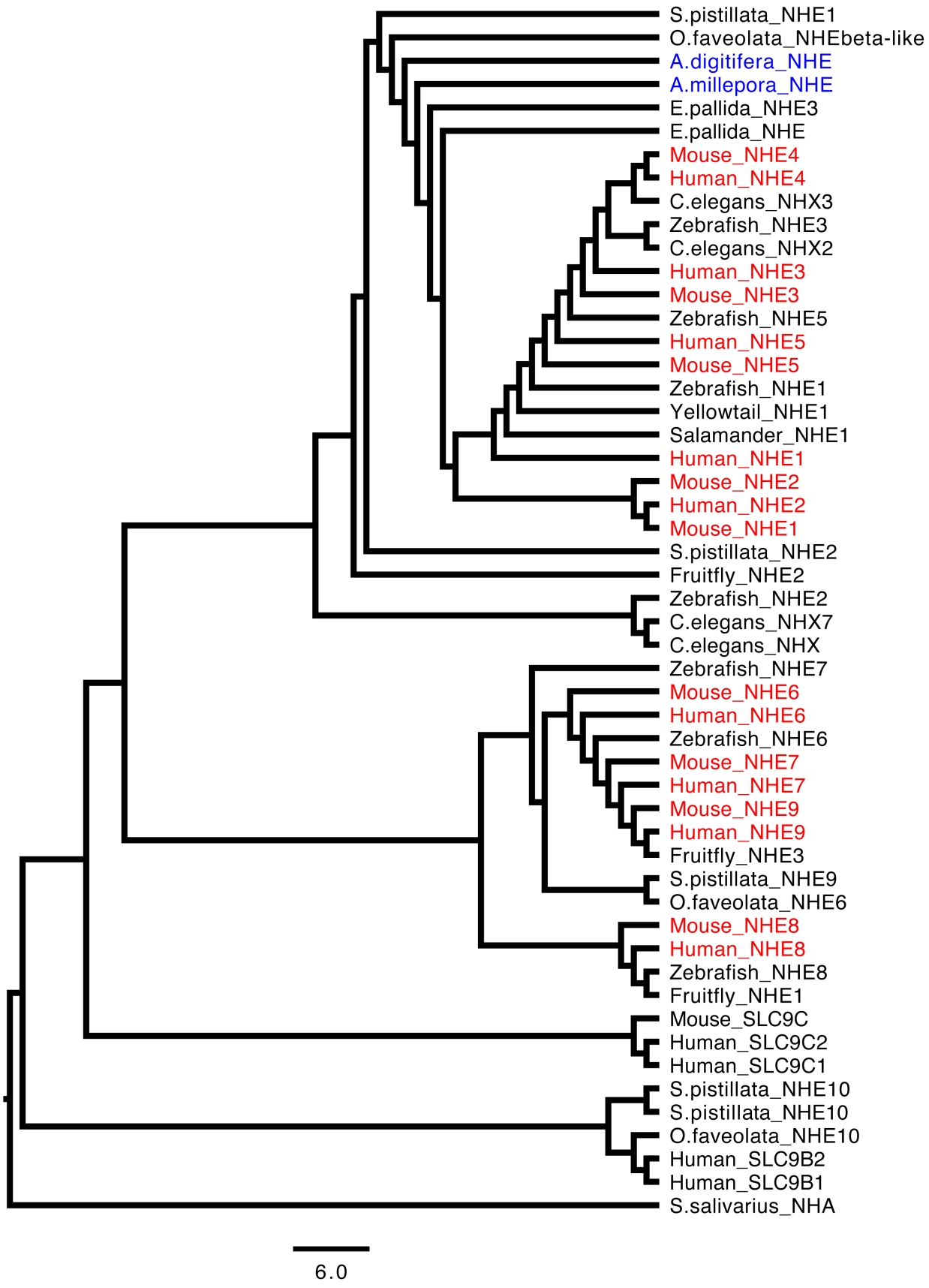
S.pistillata_NHE1
O.faveolata_NHEbeta-like
A.digitifera_NHE
A.millepora_NHE
E.pallida_NHE3
E.pallida_NHE
Mouse_NHE4
Human_NHE4
C.elegans_NHX3
Zebrafish_NHE3
C.elegans_NHX2
Human_NHE3
Mouse_NHE3
Zebrafish_NHE5
Human_NHE5
Mouse_NHE5
Zebrafish_NHE1
Yellowtail_NHE1
Salamander_NHE1
Human_NHE1
Mouse_NHE2
Human_NHE2
Mouse_NHE1
S.pistillata_NHE2
Fruitfly_NHE2
Zebrafish_NHE2
C.elegans_NHX7
C.elegans_NHX
Zebrafish_NHE7
Mouse_NHE6
Human_NHE6
Zebrafish_NHE6
Mouse_NHE7
Human_NHE7
Mouse_NHE9
Human_NHE9
Fruitfly_NHE3
S.pistillata_NHE9
O.faveolata_NHE6
Mouse_NHE8
Human_NHE8
Zebrafish_NHE8
Fruitfly_NHE1
Mouse_SLC9C
Human_SLC9C2
Human_SLC9C1
S.pistillata_NHE10
S.pistillata_NHE10
O.faveolata_NHE10
Human_SLC9B2
Human_SLC9B1
S.salivarius_NHA
6.0

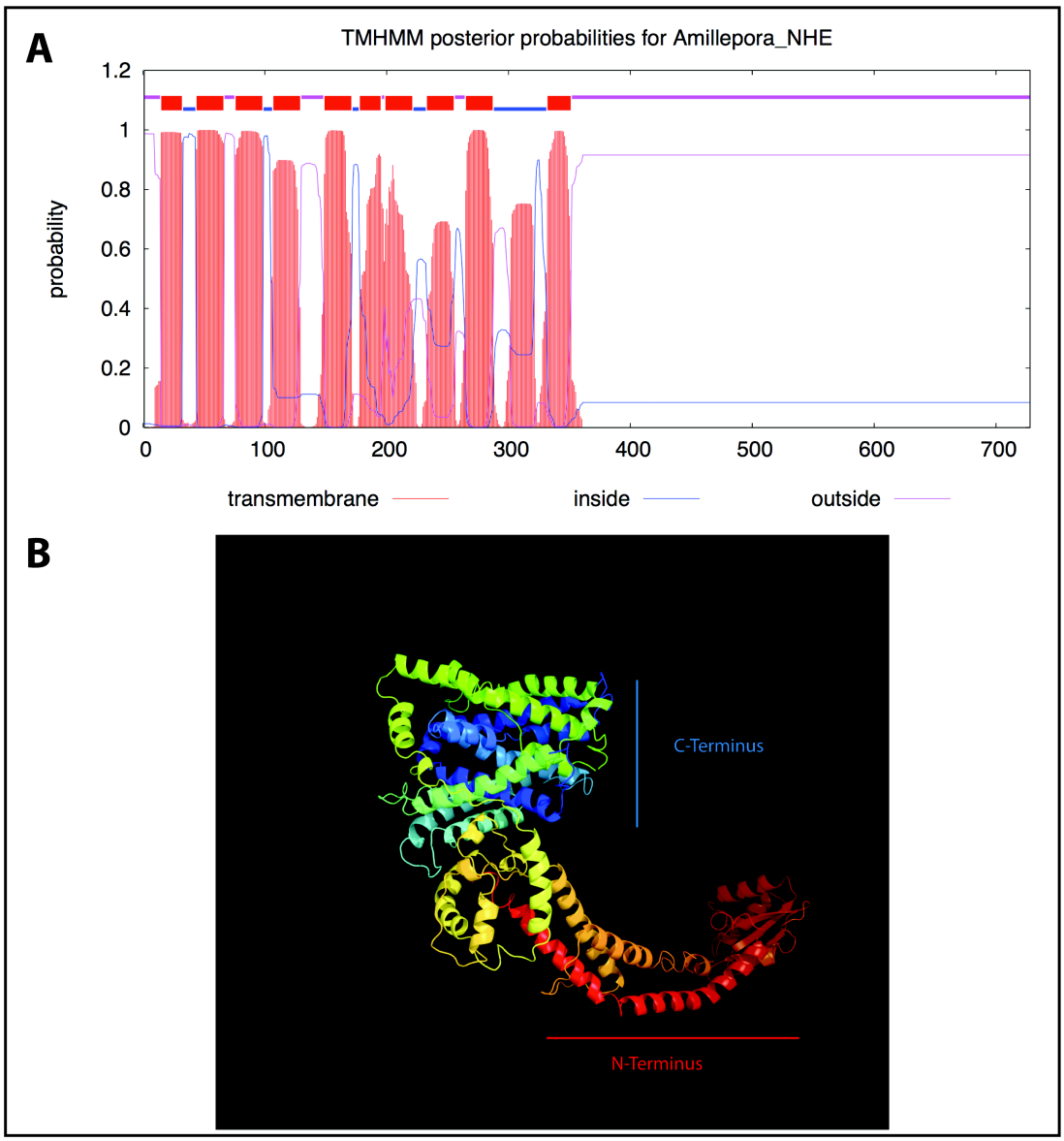

Figure 7. Predicted transmembrane regions and folding structure of *Acropora*NHE. A) Blocks of orange mark the 10 transmembrane domains, blue marks loops inside the cell and purple marks the loop outside the cell. B) A predicted 3D folded structure of coral *Acropora* NHE with C-terminus marked in blue and N-terminus marked in red.

Validation of anti-AcroporaNHE antibodies and evidence for post-translational modifications

Western blotting using anti-*Acropora*NHE antibodies detected ~52 kDa and ~114 kDa bands in *A. yongei*'s crude homogenates, and only the ~114 kDa band in the membrane protein

enriched fraction (Figure 8A). All the bands disappeared in the preabsorption peptide control (Figure 8B), indicating that the antibodies bind to the antigen epitope. Validation of the anti-*Acropora*NHE antibodies required extensive optimization, including testing several denaturing temperatures and incubation times (room temperature for 15 min, 70ºC for 15 min, 95ºC for 5 min, 90ºC for 3 min) (Appendix A), protease inhibitors (Protease Inhibitor Cocktail, PMSF, BHH and DTT) and phosphatase inhibitors (phosSTOP) at various concentrations in the homogenization buffer (Appendix B), gel running conditions (4ºC, room temperature), and the use of fresh vs. frozen coral homogenate. I also tested coral cell fractionation in an attempt to increase *Acropora*NHE abundance and facilitate its detection (Appendix C). The final protocol is described in detail in "Methods".

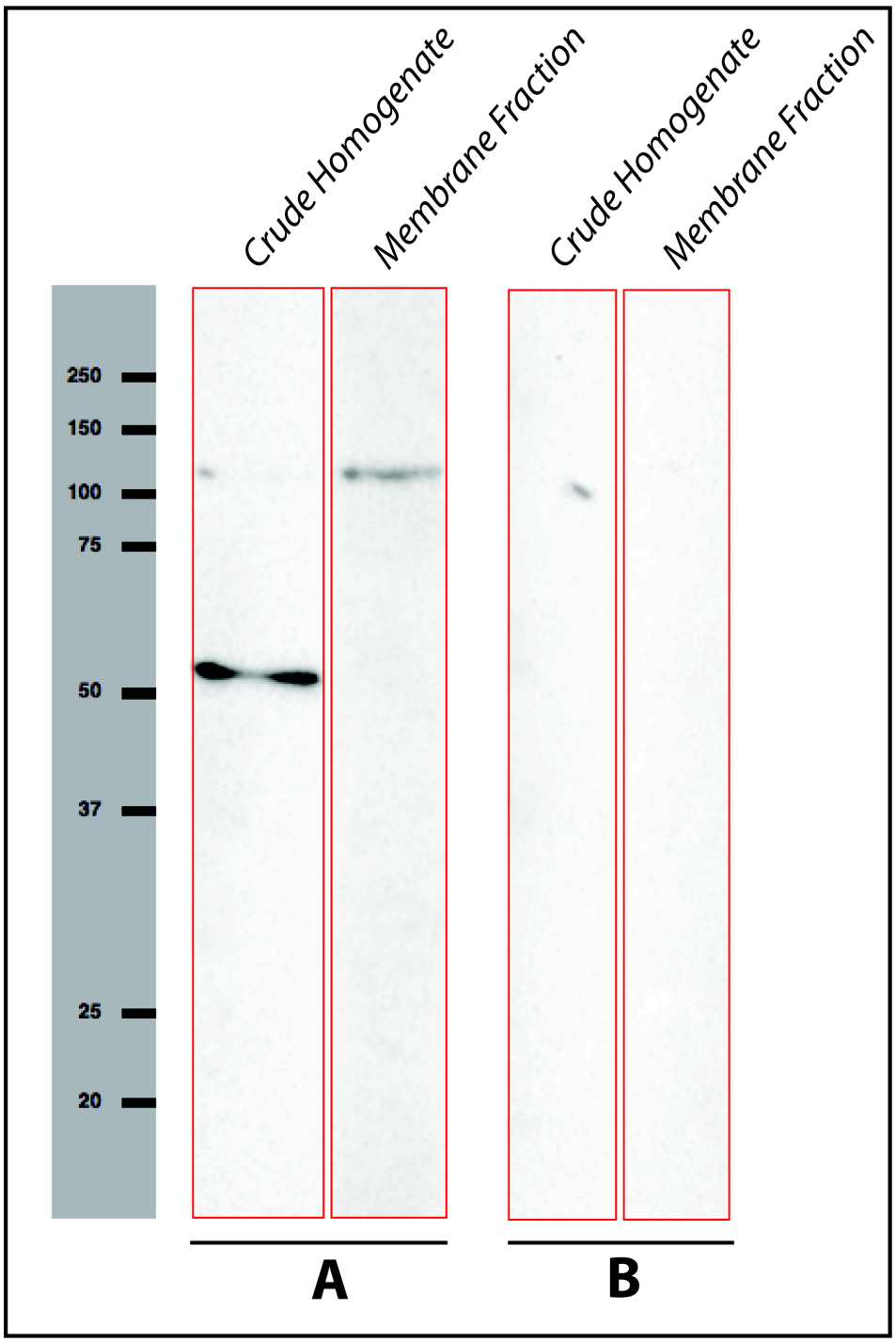

Figure 8. Identification of *Acropora*NHE by Western Blot. A) Lanes incubated with anti-*Acropora*NHE_B antibodies. B) Pre-absorption peptide control showing lack of signal in each fraction.

Although the predicted sizes of *A.millepora* NHE and *A. digitifera* NHE are respectively ~83 kDa and ~93 kDa, the two protein bands detected by Western blot were ~52 kDa and ~114 kDa. The ~52 kDa band is likely a product of proteolytic cleavage. When the three anti-*Acropora*NHE antibodies were tested, all of them recognized a ~52 kDa band, demonstrating that this smaller protein contains all three epitope regions that were used to design the anti-*Acropora*NHE antibodies (Appendix D). However, anti-*Acropora*NHE_A did not recognize the ~114 kDa band, suggesting that proteolytic cleavage may have occurred before the NHE_A epitope region, especially since smaller bands were also detected. This is evidence of proteolytic cleavage because it is much more likely for a large protein to degrade in the tissue preparation process than it is for an unrelated protein to contain all three epitope regions. Additionally, this ~52 kDa band was not recognized in the crude homogenate of every Western blot run during the optimization process (Appendix B), further indicating proteolysis during tissue processing. Proteolytic cleavage is typical for NHE isoforms from mammalian systems. For example, Western blotting of rabbit kidney yielded the ~100 kDa band predicted for NHE1, as well as a ~65-70 kDa band, that was attributed to proteolysis (Biemesderfer et al., 1992).

Alternatively, the ~52 kDa band could be a smaller coral SLC9 protein that contains the epitope regions recognized by the anti-*Acropora*NHE antibodies. Some candidates include a Cl^--dependent NHE (GenBank: AF462063.1), NHA1 and NHA2 within the *SLC9B* NHE subfamily (Donowitz et al., 2013) which are each ~52 kDa, and the mitochondrial NHA in mammalian osteoclasts, which is ~64 kDa (Battaglino et al., 2008). All of these NHE isoforms are involved in pH regulation and recovery by H^+ transport in their respective locations (Battaglino et al., 2008; Donowitz et al., 2013; Karmazyn et al., 2003; Sangan et al., 2002). However, bioinformatic analysis has not been performed in order to determine if these smaller SLC9

proteins are present in corals and whether their sequences contain the epitope regions used to develop the anti-*Acropora*NHE antibodies.

The ~114 kDa band is larger than the two predicted sizes for the *Acropora*NHE (~83 and ~93 kDa). This could be due to *A. yongei* NHE being larger than the NHE proteins from *A. millepora* and *A. digitifera.* Ongoing efforts in the Tresguerres laboratory are attempting to sequence the *A. yongei* NHE cDNA. Primers designed outside the open reading frame of the *A. millepora* NHE sequence (JT000139.1) amplified a ~2300 kb PCR product, which will be cloned and sequenced. However, the size of this potential *A.yongei* NHE encoded protein would be ~85 kDa, which is smaller than the ~114 kDa protein recognized by the anti-*Acropora*NHE antibodies.

Another explanation is post-translational modifications, such as phosphorylation and glycosylation. However, phosphorylation typically increases apparent molecular weight by 80 Da per phosphate group (McLachlin & Chait, 2001), therefore, requiring 300 and 400 phosphate groups to explain the 20-30 kDa difference between the predicted and observed sizes of *Acropora*NHE (83-93 vs ~114 kDa). As shown in Table 1, *Acropora*NHE has 63 predicted phosphorylation sites, so even if all the residues were phosphorylated (a highly unlikely possibility), phosphorylation would only account for ~5 kDa of the observed size difference.

Table 1. Predicted Glycosylation and Phosphorylation in Coral and Selected Mammalian NHEs as calculated by prediction programs outlined in "Methods".

Sequence:	Total Predicted Glycosylation Sites *	Total N-Glycosylation Predicted Sites**	Total O-Glycosylation Predicted Sites**	Total Phosphorylation Predicted Sites**
A.digitifera NHE (adi_EST_assem_7750)	45	6	39	75
*Acropora*NHE (GenBank:JT000139.1)	40	5	31	63
Rat NHE2 (L11004)	44	3	36	64
Rat NHE1 (M85299)	51	3	35	65
Human NHE1 (M81768.1)	54	3	43	70

*excluding predicted transmembrane regions
**predicted sites with >0.5 threshold score

On the other hand, the size discrepancy could be explained by glycosylation of *Acropora*NHE. When human NHE1 was deglycosylated, its size decreased from ~110 kDa to ~82 kDa, therefore glycosylation adds ~28 kDa to NHE1 (Counillon, Pouyssegur, & Reithmeier, 1994). In mammalian NHE2, deglycosylation decreased the apparent size of NHE2 from ~85kDa to ~75kDa on an SDS-PAGE gel, therefore glycosylation adds ~10kDa to NHE2 (Tse et al., 1994). Similarly, in LLC-PK cells treated with tunicamycin to inhibit glycosylation of NHE3, a ~87 kDa band was detected that was ~8 kDa smaller than the band recognized in the control lane (~95 kDa) (Soleimani et al., 1996). While glycosylation of mammalian NHE4 was not confirmed, it would explain the difference between the observed (~100 kDa) and predicted (~81 kDa) size (Bookstein et al., 1994). NHE5 is also predicted to be N-glycosylated, but it was not confirmed experimentally (Attaphitaya et al., 1999). Similarly to those mammalian NHEs, bioinformatic analysis predicts multiple potential glycosylation sites in *Acropora*NHE. Figure 9 shows predicted glycosylation sites in *A. millepora* NHE and *A.digitifera* NHE, together with human and rat NHE1, and rat NHE2 that have known glycosylation sites for comparison. Since glycosylation does not occur in hydrophobic, transmembrane regions, these regions were also

marked and excluded from the glycosylation analysis. Amino acids predicted to be glycosylated that are conserved across all five sequences are highlighted in Figure 9. Furthermore, there are two possible types of glycosylation, N- and O-glycosylation, and amino acids in *A. millepora* NHE and *A.digitifera* NHE that are predicted to be N- or O-glycosylated are summarized in Table 1.

Figure 9. NHE Sequence Alignment With Conserved, Predicted Glycosylation Sites. Two sections of an amino acid sequence alignment of *A.digitifera*NHE*, A.millepora* NHE, Rat NHE1, Rat NHE2 and Human NHE1. Purple bars indicate predicted glycosylation sites, the boxes indicate predicted glycosylation conserved across all five sequences. Green bars indicate predicted transmembrane regions. Yellow bars indicate the epitope regions used to design the anti-*Acropora*NHE antibodies (NHE_A, NHE_B, and NHE_C) in both coral sequences. Full sequence provided in Appendix E.

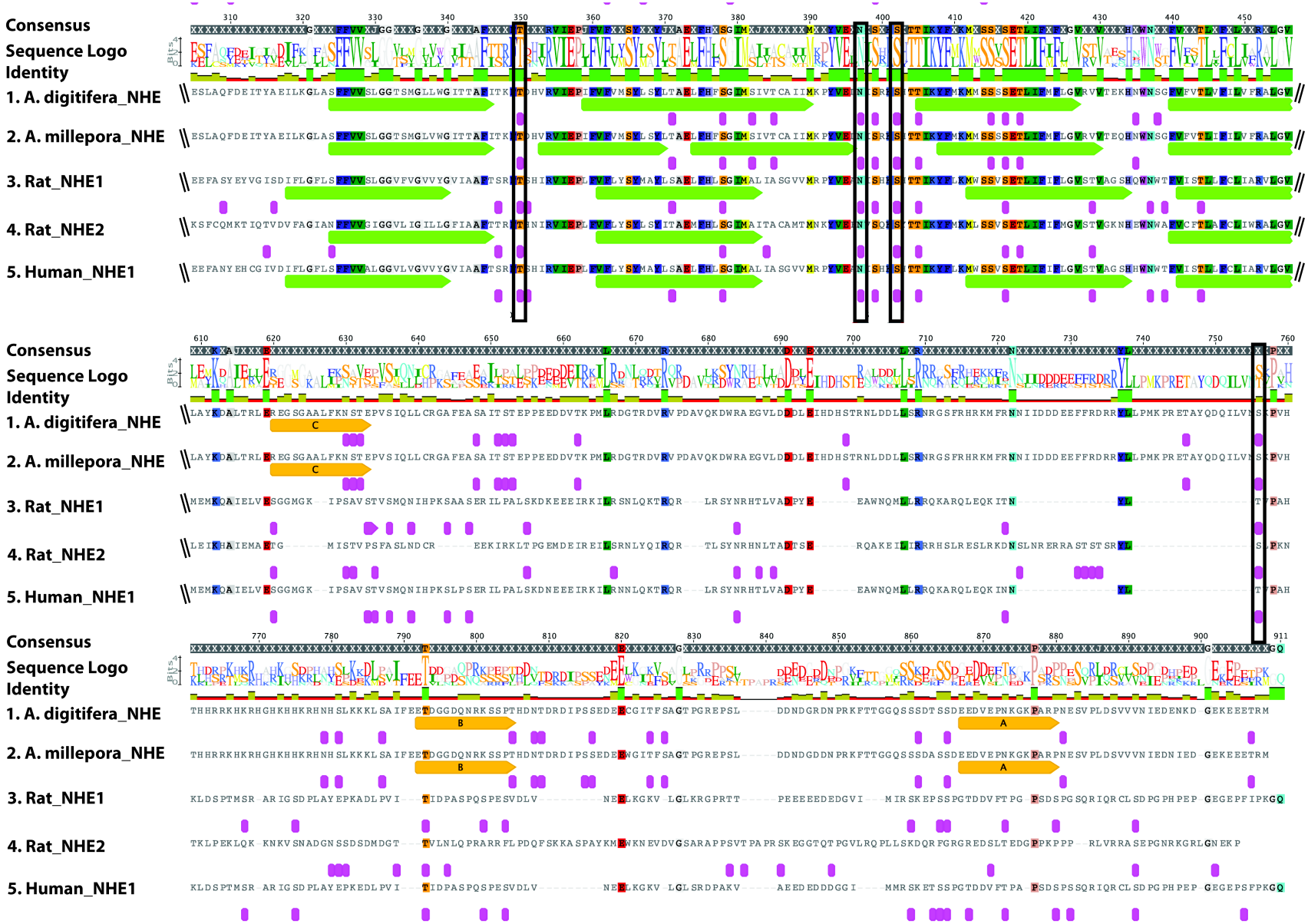
Consensus
Sequence Logo
Identity
1. A. digitifera_NHE
2. A. millepora_NHE
3. Rat_NHE1
4. Rat_NHE2
5. Human_NHE1
Consensus
Sequence Logo
Identity
1. A. digitifera_NHE
2. A. millepora_NHE
3. Rat_NHE1
4. Rat_NHE2
5. Human_NHE1
Consensus
Sequence Logo
Identity
1. A. digitifera_NHE
2. A. millepora_NHE
3. Rat_NHE1
4. Rat_NHE2
5. Human_NHE1

To test if *Acropora*NHE undergoes glycosylation, I treated coral samples with deglycosylation enzymes and ran them on an SDS-PAGE gel to detect a potential change in protein size. This step has required extreme optimization and there are still issues with the protocol that require troubleshooting. Coral samples were originally homogenized and prepared as described in "Methods" to obtain a fraction enriched in membrane proteins. Following the Non-denaturing Conditions Protocol outlined by New England BioLabs, aliquots of the membrane-enriched fraction, with and without Protein Deglycosylation Mix 2 (containing PNGase F, *O*-Glycosidase, α2-3,6,8,9 Neuraminidase A, β1-4 Galactosidase S, and β-N-acetylhexosaminidase), were incubated at 25°C for 30 min and 37°C for 16 hrs. The remaining homogenate enriched in membrane proteins was kept frozen at -80°C during the 16 hr incubation. Samples were then mixed with 4x Laemmli Buffer, denatured at 70°C for 15 min and run on an SDS-PAGE gel for analysis. The original ~114 kDa band was recognized in the lane that was not treated with the deglycosylation enzymes in Protein Mix 2, and a ~75 kDa band was recognized in the lane that was treated with the enzymes, confirming that *Acropora*NHE is glycosylated (Figure 10). The ~75 kDa band is smaller than the other two predicted sizes for NHE, however, this protocol to confirm glycosylation using the New England BioLabs Deglycosylation Mix 2 is not optimal for coral and the protocol is still being modified. Appendix F, Appendix G, and Appendix H summarizes the troubleshooting that was performed prior to achieving this result. Additional protocols for deglycosylation are being investigated, as well as alternative methods to elute, purify, and sequence the peptides found in the ~114 kDa band to further confirm it is *Acropora*NHE. It is also possible that *A. yongei* expresses a smaller NHE protein than the other two species and will be further verified by the ongoing efforts to sequence NHE in *A. yongei.*

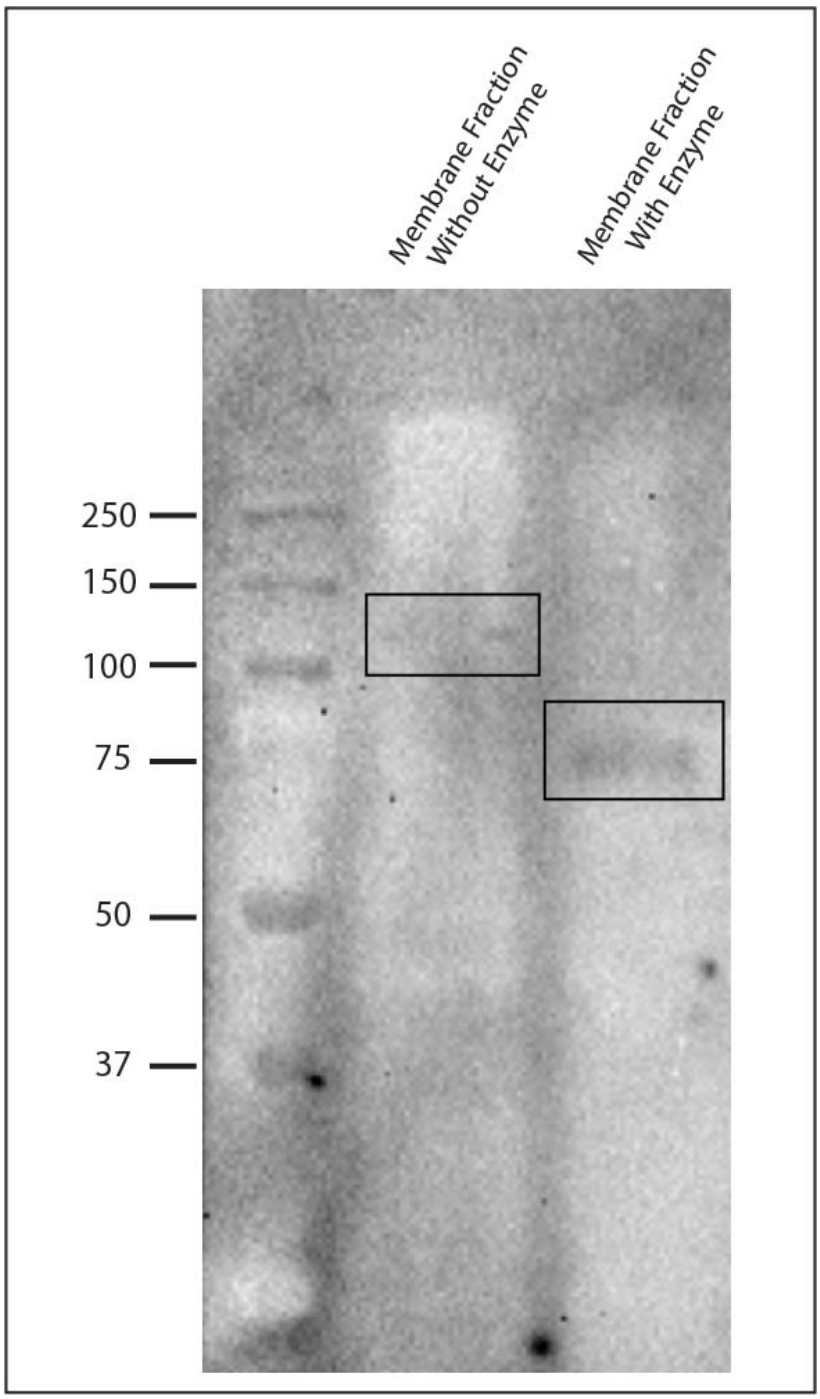

Figure 10. Deglycosylation of *Acropora*NHE. Coral samples were treated following the non-denaturing conditions protocol for the Deglycosylation Protein Mix II (New England Biolabs. A band of ~114 kDa is marked by a box in the lane containing sample that was not treated with enzymes in the Deglycosylation Protein Mix 2 and a band of ~75 kDa is marked by a box in the lane containing sample that was treated with the deglycosylation enzymes, confirming *Acropora*NHE is glycosylated.

Glycosylation and phosphorylation are very common in mammalian NHE isoforms. Glycosylation is important for proper folding of polypeptide chains (Rasmussen, 1992), for maintaining the conformation of a domain that is required for function, and to protect the protein from proteolytic attack (Feizi, 1993). Additionally, glycosylation can regulate the trafficking of proteins to the plasma membrane or intracellular compartments (Counillon et al., 1994). Human NHE1 undergoes both N- and O-linked glycosylation, yet it was determined that elimination of glycosylation did not significantly inhibit the function or biosynthesis of NHE1 (Counillon et al., 1994). Rabbit NHE2 is O-linked glycosylated, however, this glycosylation does not affect Na^+/H^+ exchanging activity (Tse et al., 1994). In human NHE3, glycosylation promotes activity and trafficking to the plasma membrane, therefore, having a functional effect (Soleimani et al., 1996). In NHE5 phosphorylation regulates activation and trafficking (Donowitz et al., 2013). Further studies are needed to determine the roles of glycosylation and phosphorylation on *Acropora*NHE. Based on the literature on mammalian NHEs, I hypothesize that glycosylation and phosphorylation regulate *Acropora*NHE trafficking from vesicles to and away from the cell plasma membrane, but they likely do not affect Na^+/H^+ exchange activity after it is present in the cell plasma membrane since functional studies have demonstrated for most NHE isoforms that deglycosylation does not inhibit the protein activity.

AcroporaNHE immunolocalization

*Acropora*NHE localization in coral tissues was examined using immunofluorescence microscopy. Based on the intense red fluorescent signal observed even at low magnification, it was immediately apparent that *Acropora*NHE was present at high abundance in the calicodermis

(Figure 11A). The anti-*Acropora*NHE$_B$ antibodies were validated for immunofluorescence by pre-absorption peptide controls, which showed only background red fluorescence from *Symbiodinium* chlorophyll (Figure 11B). At high magnification, *Acropora*NHE signal is also visible in the oral ectoderm and gastroderm of the coral tissue, albeit at much lower abundance than in the calicodermis.

Figure 11. *Acropora*NHE Immunofluoresence and Peptide Pre-absorption Control. A) *Acropora*NHE signal is abundant in the calicodermis. B) Peptide pre-absorption control. Image taken with same exposure as A. *Acropora*NHE=red; nuclei=blue; GFP and/or *Symbiodinium* chlorophyll=green. OE=oral ectoderm; OG= oral gastroderm; AG= aboral gastroderm; AE= aboral ectoderm/calicodermis; co=coelenteron; sk=skeleton.

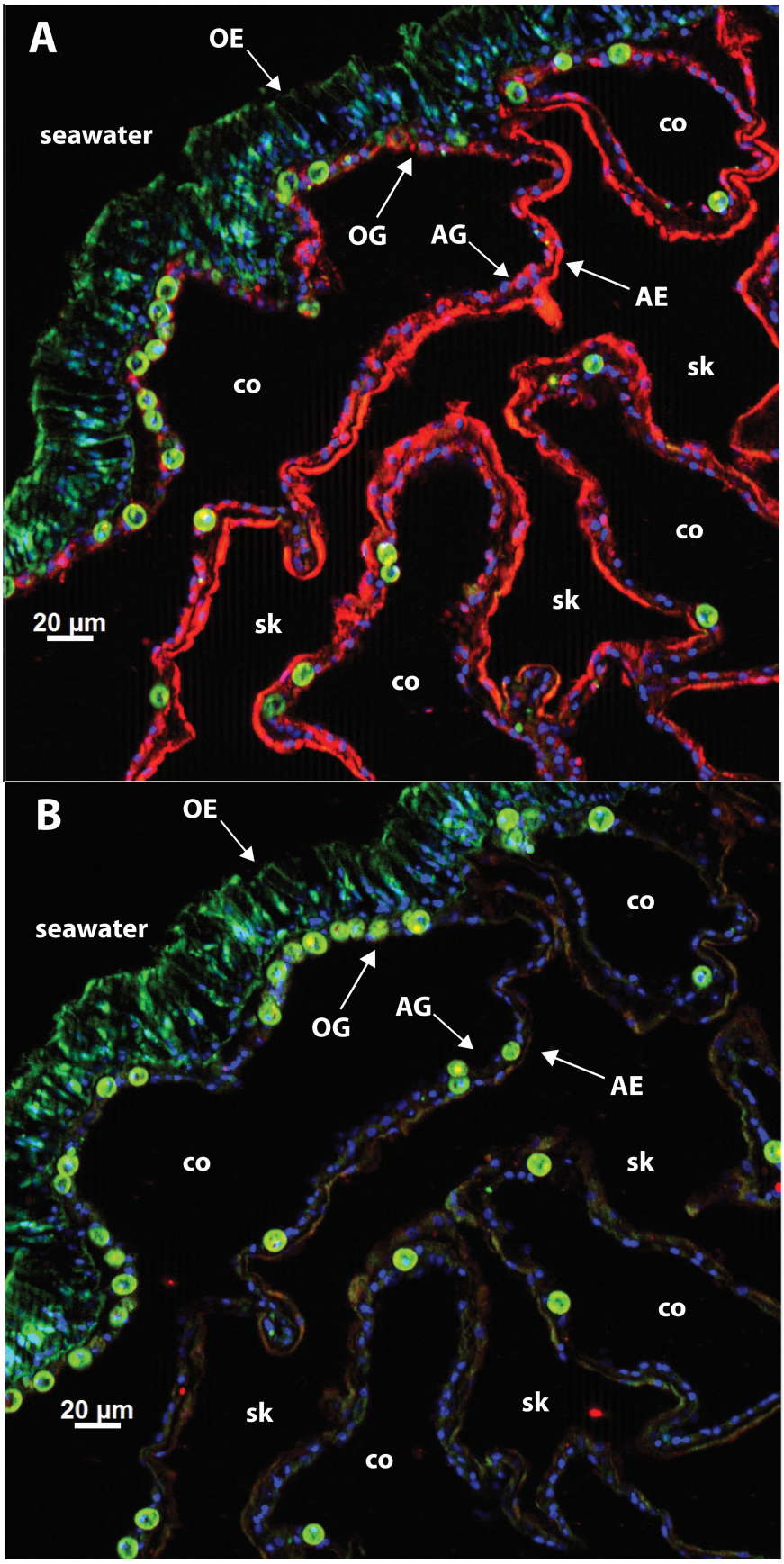
A
OE
seawater
co
OG
AG
AE
sk
co
co
sk
sk
20 µm
co
B
OE
seawater
co
OG
AG
AE
co
sk
co
20 µm
sk
sk
co

In two of the four samples analyzed, *Acropora*NHE was occasionally present in the apical membrane of oral ectodermal cells (Figure 12A). Since the oral ectoderm is in contact with the seawater, *Acropora*NHE could be involved in secreting H^+ for pHi regulation to counterbalance the effects of metabolic acid/base disturbances or of fluctuating pH in the surrounding environment. The *Acropora*NHE signal could also be due to localization in lysosomes and endosomes.

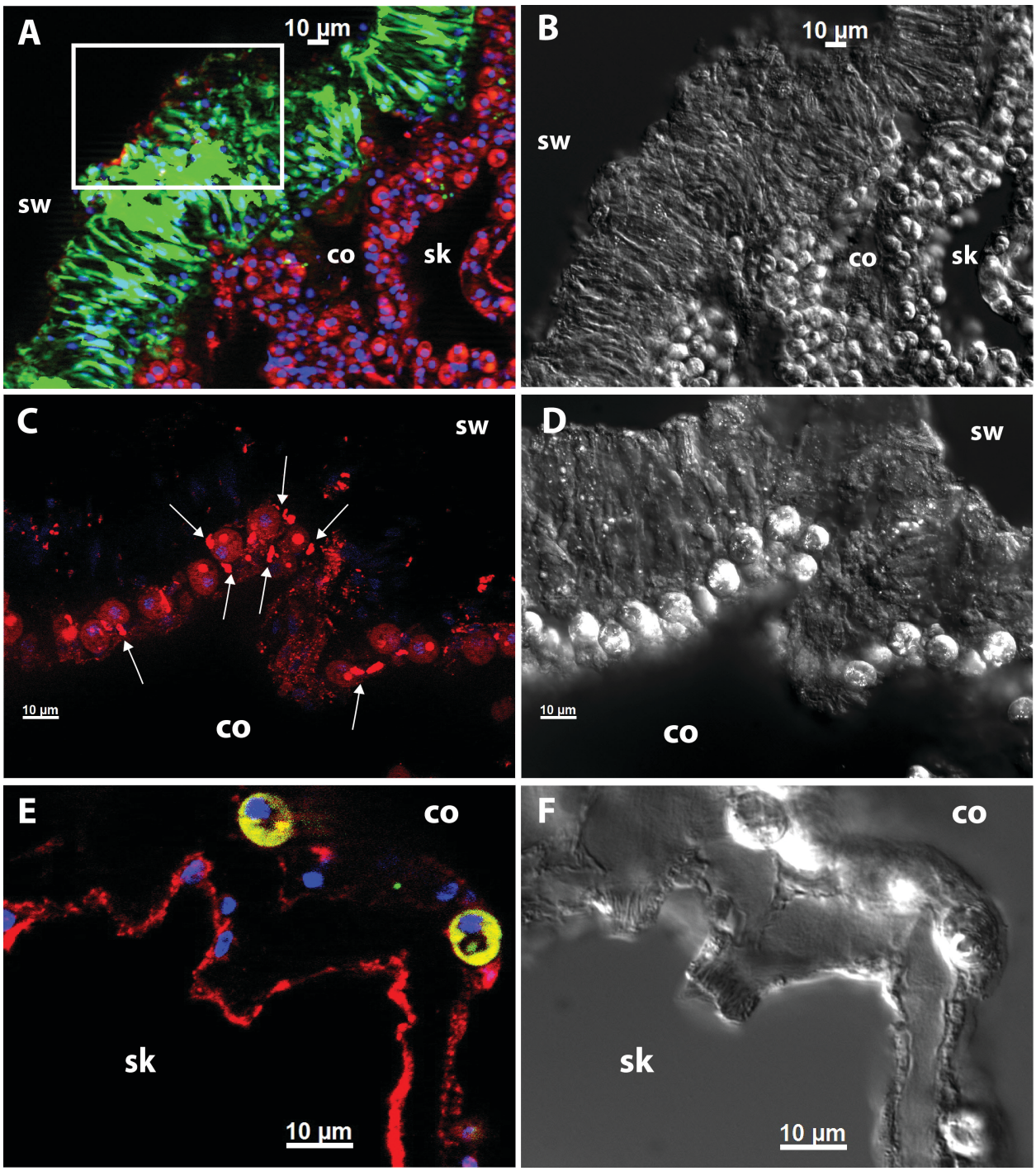

Figure 12. *Acropora*NHE localization in the oral ectoderm, in symbiocytes and in desmocytes. A) *Acropora*NHE in the apical membrane of the oral ectodermal cells circled by the box. B) DIC image showing tissue morphology of A. C) *Acropora*NHE localizing to specific compartments in the symbiocyte cells, marked by arrows. D) DIC image showing tissue morphology of C. E) *Acropora*NHE in the desmocytes. F) DIC image showing tissue morphology of E. In Images A, C, and E *Acropora*NHE=red; nuclei=blue; GFP and/or *Symbiodinium* chlorophyll=green. sw=seawater; co=coelenteron; sk=skeleton.

At high magnification, in all four samples, *Acropora*NHE was evident in small aggregates within the gastrodermal cells with and without *Symbiodinium* (Figure 12C). However, these aggregates were particularly evident in the symbiocytes. I hypothesize these aggregates correspond to organelles, most likely the endoplasmic reticulum and the Golgi apparatus, seeing as these organelles are involved in protein modification and trafficking. Organelles that are involved in secretory and endocytic pathways have a weak acidity in their lumen; for example, the trans-Golgi network pH is ~6. The Golgi apparatus and endoplasmic reticulum play an important role in protein glycosylation, while also preparing proteins in vesicles to be trafficked throughout the cell. However, *Acropora*NHE is more similar to the mammalian NHEs 1-5 that are typically present in the cell plasma membrane than to the mammalian intracellular NHE 6-9 found in the Golgi, trans-Golgi and the Endoplasmic Reticulum (Nakamura et al., 2005). A more likely explanation is that the signal could be due to *Acropora*NHE in the Golgi as it is being glycosylated and packaged in vesicles. Since this localization was not observed in other cell types, it might be related to a function that is specific to symbiocytes. For example, gastrodermal cells must synthesize and maintain the symbiosome membrane and some of the associated proteins are likely to require glycosylation. Additionally, this signal could be related to lysosomes and endosomes in cell digestive and recycling pathways that could be upregulated in order to maintain the symbiosis. The potential *Acropora*NHE presence in the Golgi apparatus could be verified by co-immunostaining with the Golgi marker antibody, GM-130; however, this tool (like most cellular and molecular biology tools) were designed for mammalian cells so they will need to be validated for coral cells.

*Acropora*NHE is most abundant in the two cell types in the calicodermis: desmocytes and calicoblastic cells. In desmocytes, *Acropora*NHE signal is present along the basolateral

membrane (Figure 12E). In calicoblastic cells, *Acropora*NHE signal was the strongest (Figure 13). Due to the overlapping and interweaving arrangement of calicoblastic cells, I was not able to determine whether *Acropora*NHE is localized to the apical membrane, the basolateral membrane, or in vesicles throughout the cell cytoplasm. The most likely location is in the basolateral membrane where *Acropora*NHE would help remove H^+ from the SCM by secreting H^+ out of the calicoblastic cells, into the mesoglea and eventually the aboral gastroderm and coelenteron (Figure 14). Calicoblastic cells also express high levels of NKA (Barrot et al., 2015a), which would provide the driving force for *Acropora*NHE activity.

If *Acropora*NHE is present in vesicles, it could assist in cell digesting or recycling pathways, or contribute to vesicular ACC formation. Also, *Acropora*NHE could be present in vesicles as they are trafficked to and inserted in the basolateral membrane. *Acropora*NHE localization in the apical membrane is unlikely because NHEs transport Na^+ into cells and H^+ out of cells, and therefore *Acropora*NHE activity would acidify the SCM and impair biomineralization.

Figure 13. *Acropora*NHE in the calicoblastic cells. A) Low magnification of all four tissue layers showing the *Acropora*NHE the calicodermis. This can be differentiated from the red fluorescent signal of chlorophyll present in the *Symbiodinium* using negative and pre-absorption peptide controls. B) High magnification of calicoblastic cells. *Acropora*NHE=red; nuclei=blue; GFP and/or *Symbiodinium* chlorophyll=green.

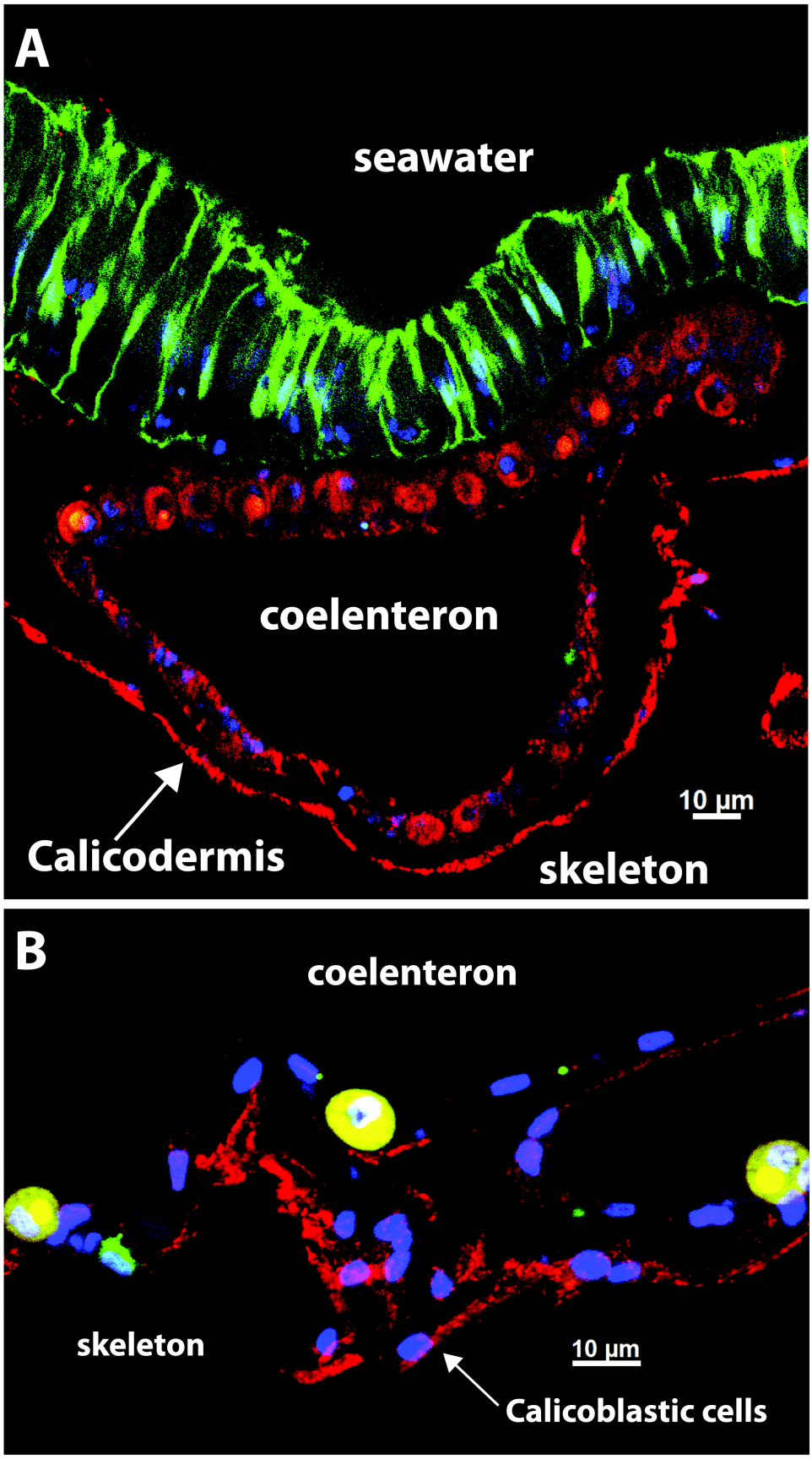
A
seawater
coelenteron
Calicodermis
10 µm
skeleton
B
coelenteron
skeleton
10 µm
Calicoblastic cells

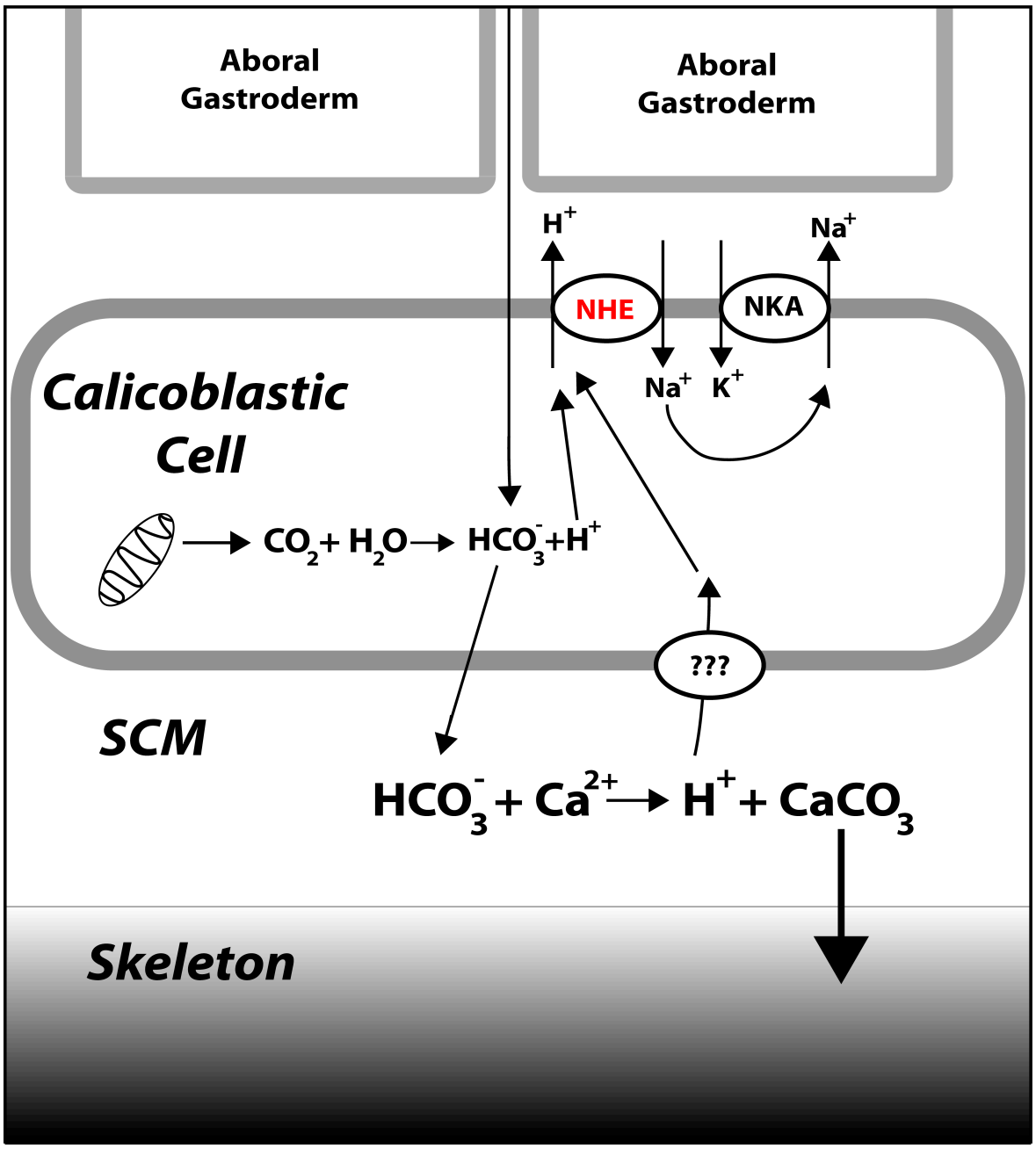

Figure 14: Potential Role of *Acropora*NHE and NKA in calicoblastic cells. Na^+/K^+-ATPase (NKA) keeps $[Na^+]$ low in the cell that drives H^+ secretion by *Acropora*NHE (NHE). CO_2 is produced by aerobic respiration in mitochondria, which is hydrated into HCO_3^- and H^+ in the cytoplasm. The H^+ is transported out of the cell by NHE in order to maintain pHi, while the metabolically-produced and externally-sourced HCO_3^- is transported to the SCM for calcification. As $CaCO_3$ is crystallized, H^+ is produced, transported into the calicoblastic cells by an unknown mechanism, and removed by NHE.

*Acropora*NHE immunolocalization in calicoblastic cells was further analyzed in regions known to calcify at different rates. Areas of rapid calcification were identified based on the presence of only two tissue layers, the oral ectoderm and calicodermis (Figure 15). Two regions of rapid calcification were present in *A. yongei*: the tip of the branch (Figure 15A, 15B, 15C), and spicules or growing side branches at the middle and base of the branch (Figure 15D). However, I found no qualitative differences in *Acropora*NHE localization or abundance in calicoblastic cells between areas of rapid calcification and the rest of the branch. This suggests that *Acropora*NHE is involved in both rapid calcification for branch extension and growth and in maintaining already built skeleton.

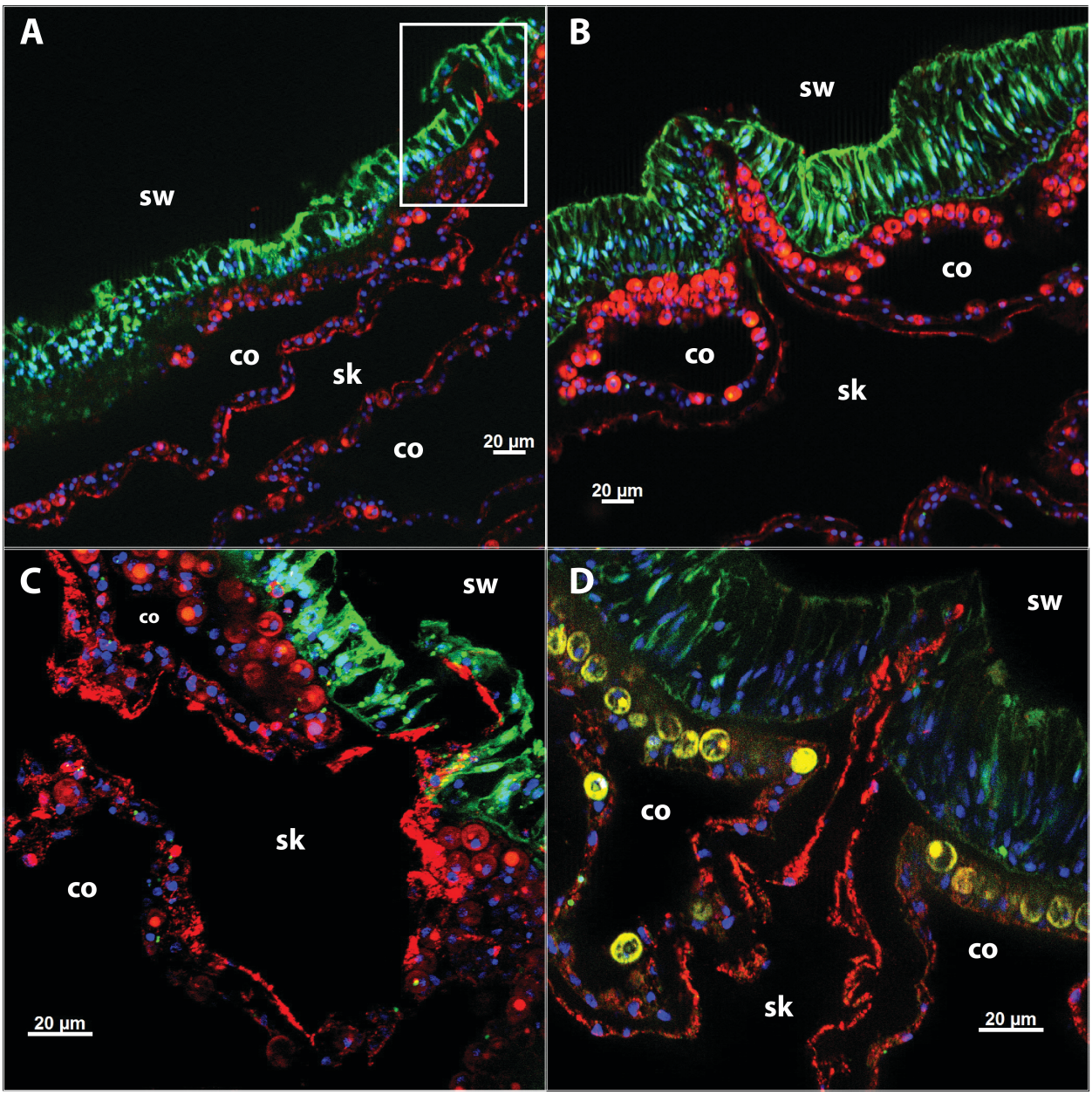

Figure 15. NHE localized to the calicoblastic cells in regions of rapid calcification. A) Tissue near the tip of a branch. The box indicates lack of gastrodermal layers characteristic of areas of rapid calcification. B) Tissue near the tip of a branch indicates lack of gastrodermal layers characteristic of areas of rapid calcification. C) Magnification of the box area from Image A. D) Magnification of an area of rapid calcification from the base of the branch with no gastrodermal layers. *Acropora*NHE=red; nuclei=blue; GFP and/or *Symbiodinium* chlorophyll=green. OE=oral ectoderm; OG= oral gastroderm. sw= seawater; co= coelenteron; sk= skeleton.

Future Work

Further work is needed to determine *Acropora*NHE subcellular localizations in various cell types and to elucidate its associated physiological functions. One limitation of immunolocalization studies using tissue sections is a potential alteration of the morphology of calicoblastic cells as a result of fixation, paraffin embedding and sectioning. Immunolocalization on coral microcolonies growing on glass coverslips (Venn et al., 2011) could help circumvent that limitation because there would no longer be a need to embed in paraffin or section, potentially maintaining the structure of the calicoblastic cells and the SCM. Thus, immunostaining of coral microcolonies could result in a more accurate determination of *Acropora*NHE subcellular localization in calicoblastic cells and provide further insight into coral calcification mechanisms. Microcolonies have only been used to image live coral samples thus far, therefore, optimization of fixation and immunofluorescence staining protocols would be required.

Coral microcolonies could also help determine the physiological function of *Acropora*NHE in calicoblastic cells. Using this setup, Venn et al. (2011) characterized the pH in calicoblastic cells and pHe in the SCM using the ratiometric pH-sensitive dyes SNARF-1 and SNARF-1 AM. A potential role of *Acropora*NHE in pHi regulation in calicoblastic cells could be tested in a similar manner through addition of pharmacological inhibitors specific for NHEs such as amiloride, cariporide and EIPA (reviewed by Xu et al., 2018). I predict NHE inhibitors will result in pHi and pHe acidification, indicating *Acropora*NHE is involved in pHi regulation of calicoblastic cells and in removing H^+ from the SCM.

The high abundance of *Acropora*NHE in calicoblastic cells opens new opportunities for studying coral cell biology. For example, when epithelial cells are isolated, they lose their polarity and shape, which complicates identifying each cell type. Until now, studies on isolated cells have been limited to symbiocytes and cnidocytes, which are the only identifiable cell types due to the presence of *Symbiodinium* (Barott et al., 2015b) and the nematocyst (Basulto et al., 2006), respectively. The anti-*Acropora*NHE antibodies validated in this thesis can now be used as specific markers for calicoblastic cells in isolated coral cell preparations, providing more tools for future studies about coral calcification mechanisms at the cellular level.

The potential roles of *Acropora*NHE in pHi regulation in calicoblatic cells and in H^+ removal from the SCM to promote calcification could be relevant for understanding corals' responses to ocean acidification (OA). OA is the predicted decrease in the pH of the surface open ocean due to an increase in the concentration of CO_2 resulting from human industrial activities. Many studies have predicted that OA will decrease the availability of CO_3^{2-} in seawater and impair coral calcification. However, while decreased calcification rates have indeed been observed in some coral species (Putnam et al., 2016), the reasons are not clear because the skeleton is not in direct contact with seawater and calcification takes place in the SCM under coral control (Allemand et al., 2004). Furthermore, other studies have concluded that seawater $[CO_3^{2-}]$ does not affect calcification (Jokiel, 2013), likely because the DIC necessary for calcification might be HCO_3^- from seawater and from metabolic origin (after CO_2 hydration) and not from CO_3^- (Comeau et al., 2013). Alternatively, OA could affect coral calcification due to the increase in seawater $[H^+]$ (reduced pH). As the gradient between intracellular and environmental $[H^+]$ decreases, H^+ removal from the SCM could become more energetically costly (Jokiel, 2013; Ries, 2011). This "proton flux model" may explain a decrease in calcification rates in some

experimentally induced OA-like studies (Jokeil, 2013; Ries, 2011). The magnitude of this effect would be dependent on the coral pHi regulatory mechanisms, the efficacy of their H^+ removal pathways, and their ability to supply the energy required for those pathways (Ries, 2011). Importantly, the relevant extracellular compartment is the coelenteron and not seawater. Since the mechanisms for H^+ removal from the SCM may be species-specific, they could determine vulnerability and resilience to OA. This emphasizes the importance of further elucidating coral cellular mechanisms that control pH regulation and calcification, such as the characterization of NHEs in multiple coral species.

The effects of OA on calicoblastic pHi regulation, H^+ removal from the SCM and the potential involvement of NHEs could be studied in coral microcolonies as described earlier. In *S. pistillata* microcolonies, Venn et al. (2013) demonstrated that there was significant decline in the pH of the SCM with increases in seawater acidification. Coral microcolonies can be used to study the role of NHEs in regulating the pHi of the calicoblastic cells and the pH of the SCM during OA conditions using pH sensitive dies. I predict NHE inhibitors will induce even greater pH differences in the SCM.

In summary, I have identified SLC9 proteins in several coral species. For the first time, I have provided a characterization of a coral NHE protein, specifically *Acropora*NHE's membrane topology and identified potential phosphorylation and glycosylation sites. I validated anti-*Acropora*NHE antibodies for Western blotting and found that the molecular size of *Acropora*NHE protein from *A. yongei* tissues was larger than predicted due to glycosylation. Ongoing studies are examining potential glycosylation effects on *Acropora*NHE protein size. I also validated anti-*Acropora*NHE antibodies for immunohistochemistry; *Acropora*NHE was abundantly present in calicoblastic cells, suggesting roles in pHi regulation and in H^+ removal

from the SCM. The specific mechanisms used by coral to maintain an alkaline pH at the site of calcification, as well as, maintain the intracellular pH of the calicoblastic cells, to-date, is not known. The identification of an NHE protein in these coral cells provides a starting point to further investigate and gain understanding about the cellular and molecular mechanisms of coral biomineralization. The use of anti-*Acropora*NHE antibodies could be used as a novel marker for calicoblastic cells in future studies to investigate coral calcification at the cellular level. The characterization of *Acropora*NHE also opens the door for future work to elucidate its function in other coral cell types and for identification and functional analysis of NHE in other coral species. Ultimately, all that information will lead to more accurate predictions of how coral will respond to environmental challenges, such as ocean acidification.

This thesis is being prepared for submission for publication of the material. Ortega, Mikayla; Tresguerres, Martin. Ms. Ortega was the primary investigator and author of this material.

APPENDIX A

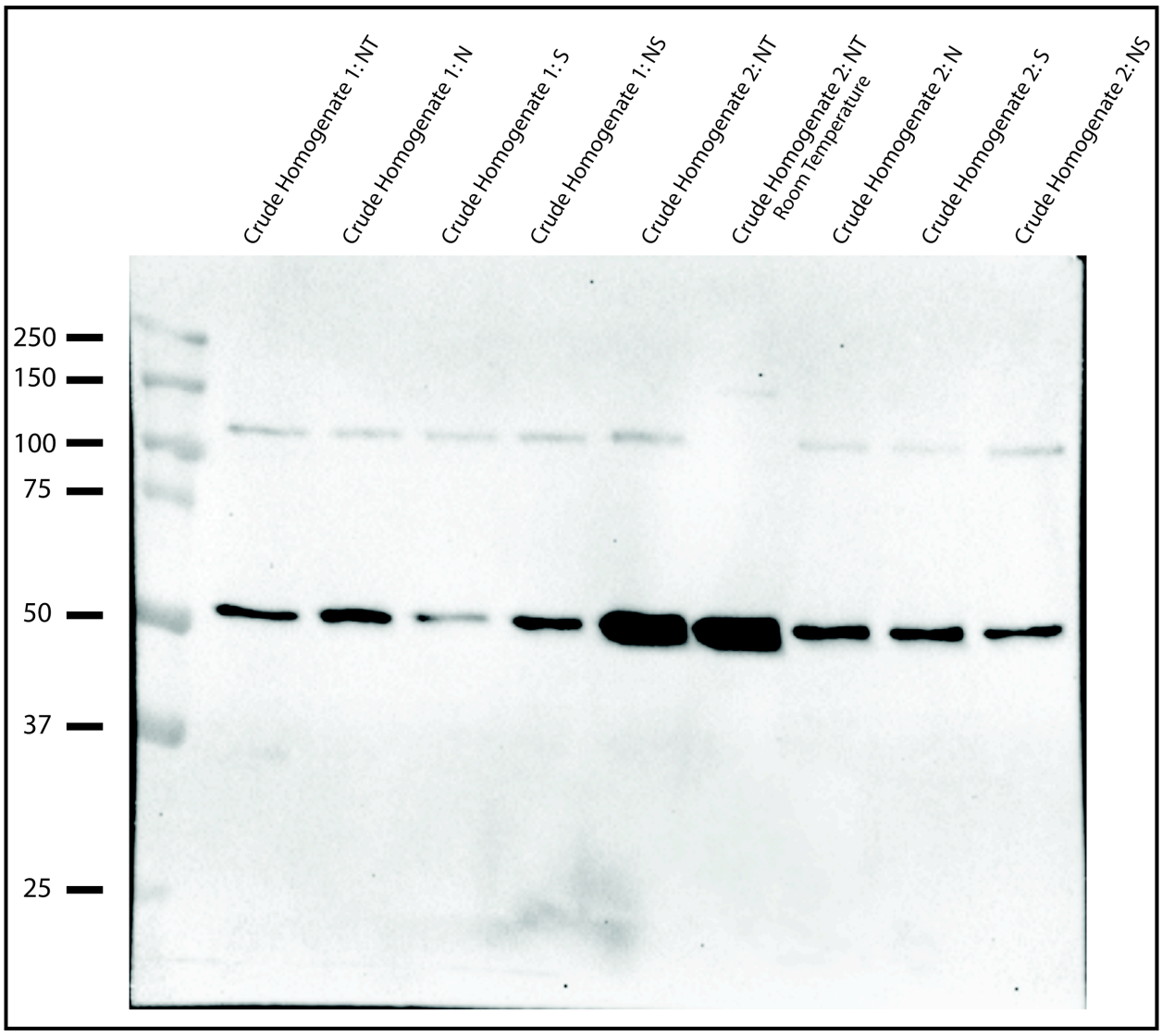

Figure 16. Optimization of anti-*Acropora*NHE$_B$ antibodies: Effect of Temperature. Coral homogenate was sheared in one of three ways: passing through a needle and syringe, ultrasonication, or a combination of both. Crude homogenate, with and without *Symbiodinium*, aliquots were either not treated or processed with one of these three shearing methods. Each sample was then denatured at either 70ºC, except for one lane that was denatured at room temperature for 15 min (indicated in the image). The gel was transferred to a PVDF membrane, and incubated with anti-*Acropora*NHE$_B$ antibodies. Crude Homogenate 1 contains *Symbiodinium*, while Crude Homogenate 2 does not. NT=no treatment, N=sheared by needle and syringe, S=sheared by ultrasonication, NS=sheared by a combination of both methods. The different shearing methods did not appear to yield different results.

APPENDIX B

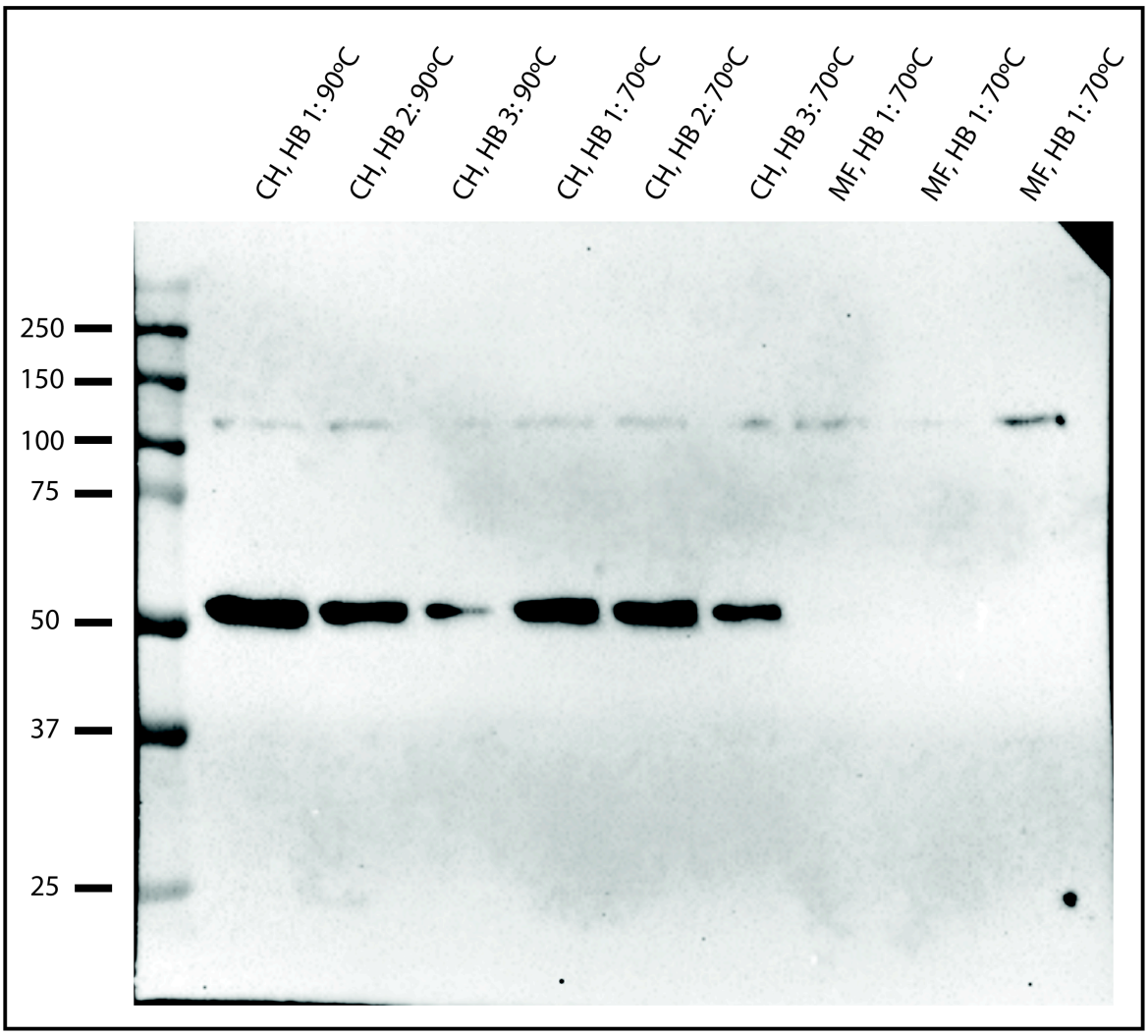

Figure 17. Optimization of anti-*Acropora*NHE$_B$ antibodies: Effect of Homogenization Buffer. Three different coral branches cut from the same colony were homogenized using an airbrush with three different homogenization buffers. Samples of Crude Homogenate, without *Symbiodinium*, and fractionated membrane proteins were loaded into each lane. Each Crude Homogenate lane contains 15 µg of protein while the Membrane Fraction lanes contain 14 µg of protein. Homogenization Buffer 1 contains S22 Buffer + 10xPIC + 10xPhosStop; Homogenization Buffer 2 contains S22 Buffer + 10xPIC + 10xPhosStop + PMSF +BHH; Homogenization Buffer 3 contains S22 Buffer + PMSF + BHH + DTT. The three Crude Homogenate samples were denatured under two different treatments: 90ºC for 3 min, 70ºC for 15 min; the Membrane Fractions were denatured at 70ºC for 15 min. The temperature each lane was treated with is indicated in the image. The SDS-PAGE gel was transferred to a PVDF membrane and treated with anti-*Acropora*NHE$_B$ antibodies. CH=Crude Homogenate, HB=Homogenization Buffer, MF=Membrane Fraction.

APPENDIX C

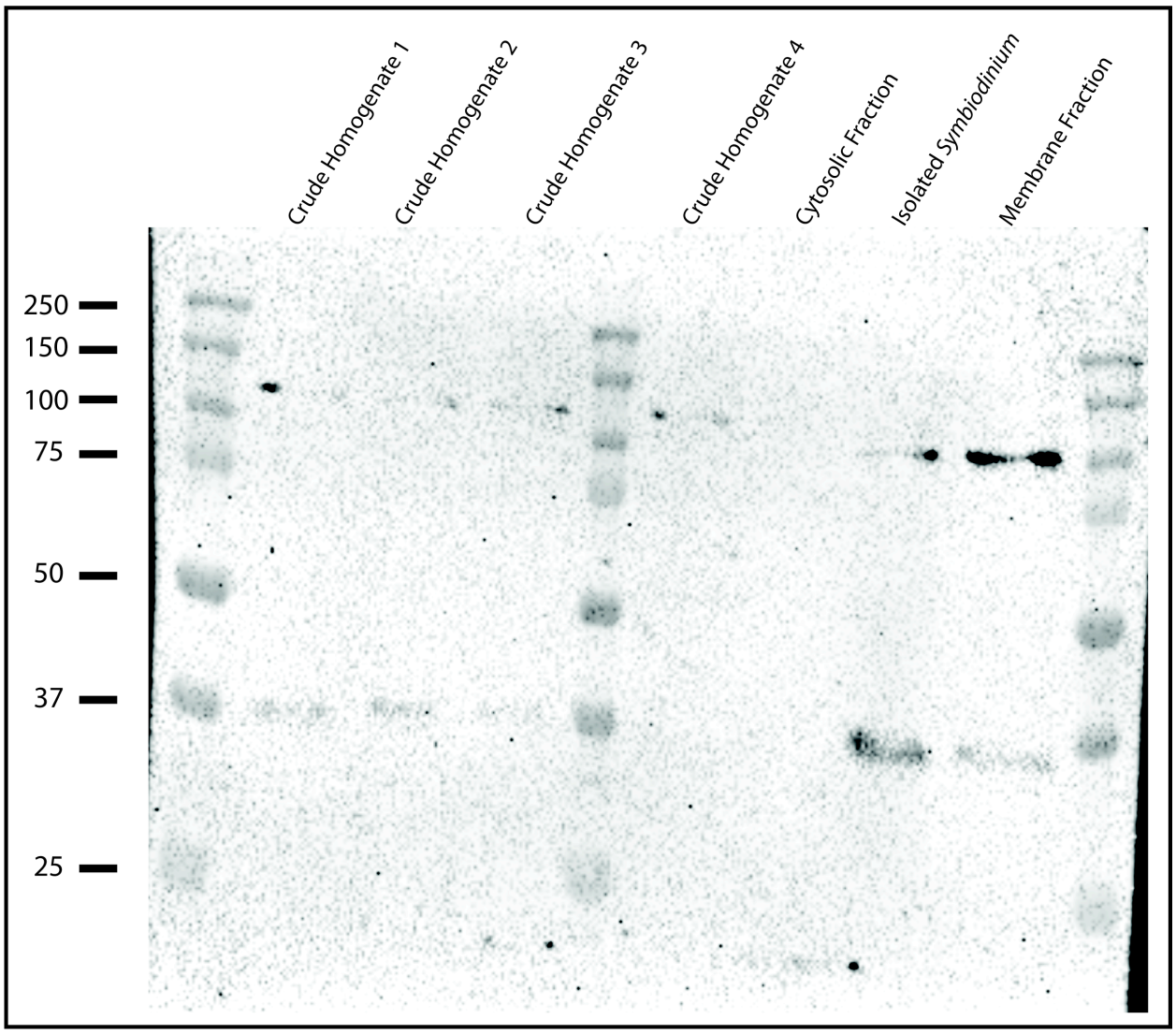

Figure 18. Optimization of anti-*Acropora*NHE$_B$ antibodies: Fractionation. Aliquots of homogenate were taken at different steps of the fractionation protocol and loaded into a SDS-PAGE gel. Crude Homogenate 1, 2, and 3 contain *Symbiodinium*. Crude Homogenate 2 was sheared with a needle and syringe; Crude Homogenate 3 was sheared with a needle and syringe and ultrasonicated; Crude Homogenate 4 does not contain *Symbiodinium.* The homogenate was then further fractioned into Isolated *Symbiodinium*, Membrane Fraction, and Cytosolic Fraction. The gel was transferred to a PVDF membrane and treated with the anti-*Acropora*NHE$_B$ antibody. Crude Homogenate 4 revealed a single band ~114 kDa, while the Membrane Fraction revealed a ~114 kDa band as well as a ~23 kDa band.

APPENDIX D

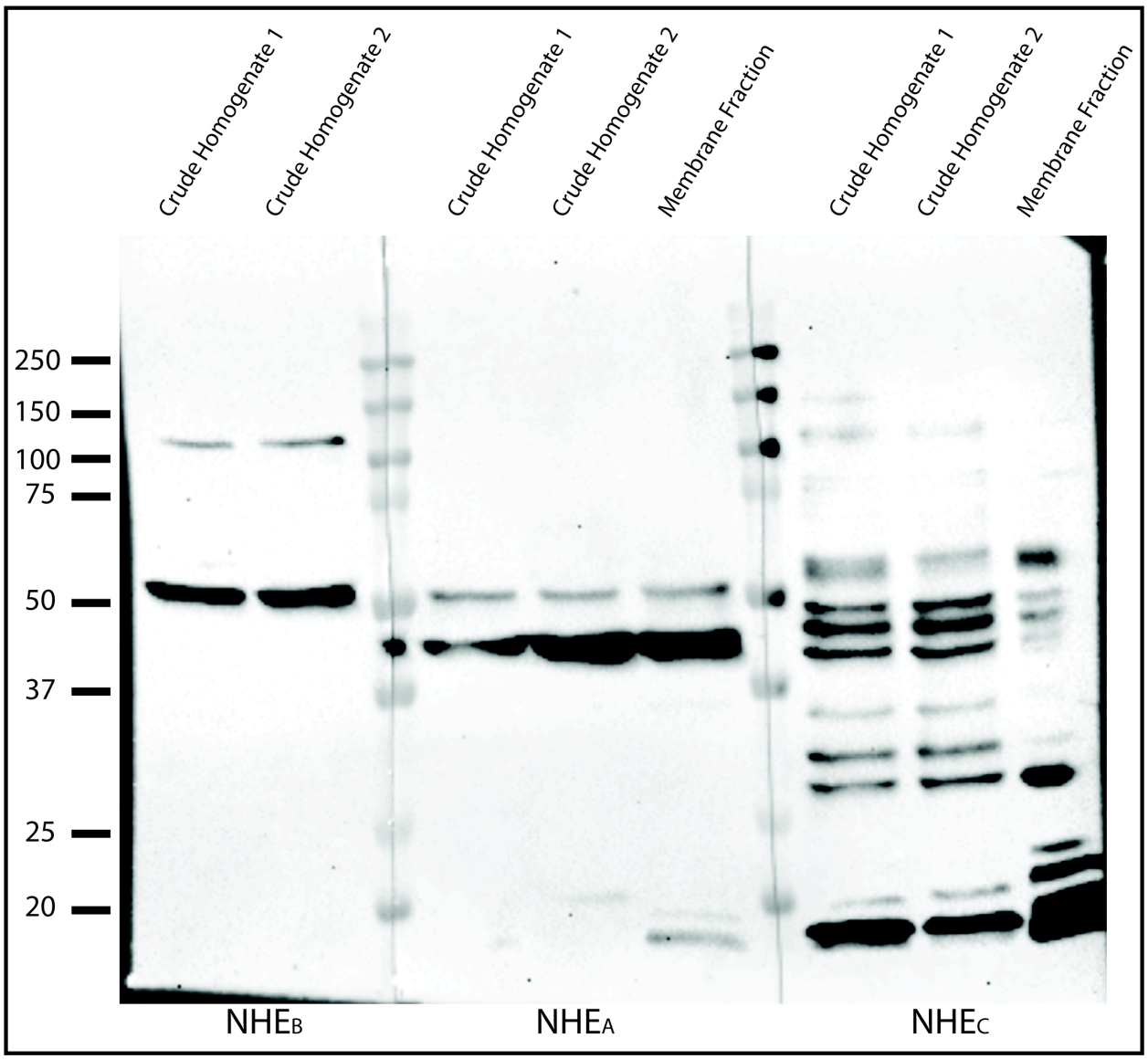

Figure 19. Validation of three anti-*Acropora*NHE antibodies. Coral homogenate samples from the same branch were loaded into an SDS-PAGE gel at the same protein concentration (Crude Homogenates=15µg, Membrane Fraction=23 µg). Crude Homogenate 1 contains *Symbiodinium*, while Crude Homogenate 2 does not. After transferring to a PVDF membrane, the same volume and concentration of NHE_A, NHE_B, and NHE_C were tested. All three antibodies identified a band ~52 kDa.

Figure 20. Complete sequence alignment of *A. digitifera* NHE, *A. millepora* NHE, Rate NHE1, Rat NHE2, and Human NHE1. Four amino acids predicted to be glycosylated across all 5 sequences circled by boxes. Green bars= predicted transmembrane regions; pink bars=predicted glycosylation sites; Yellow bars= epitope regions for used to design anti-*Acropoora*NHE antibodies.

APPENDIX F

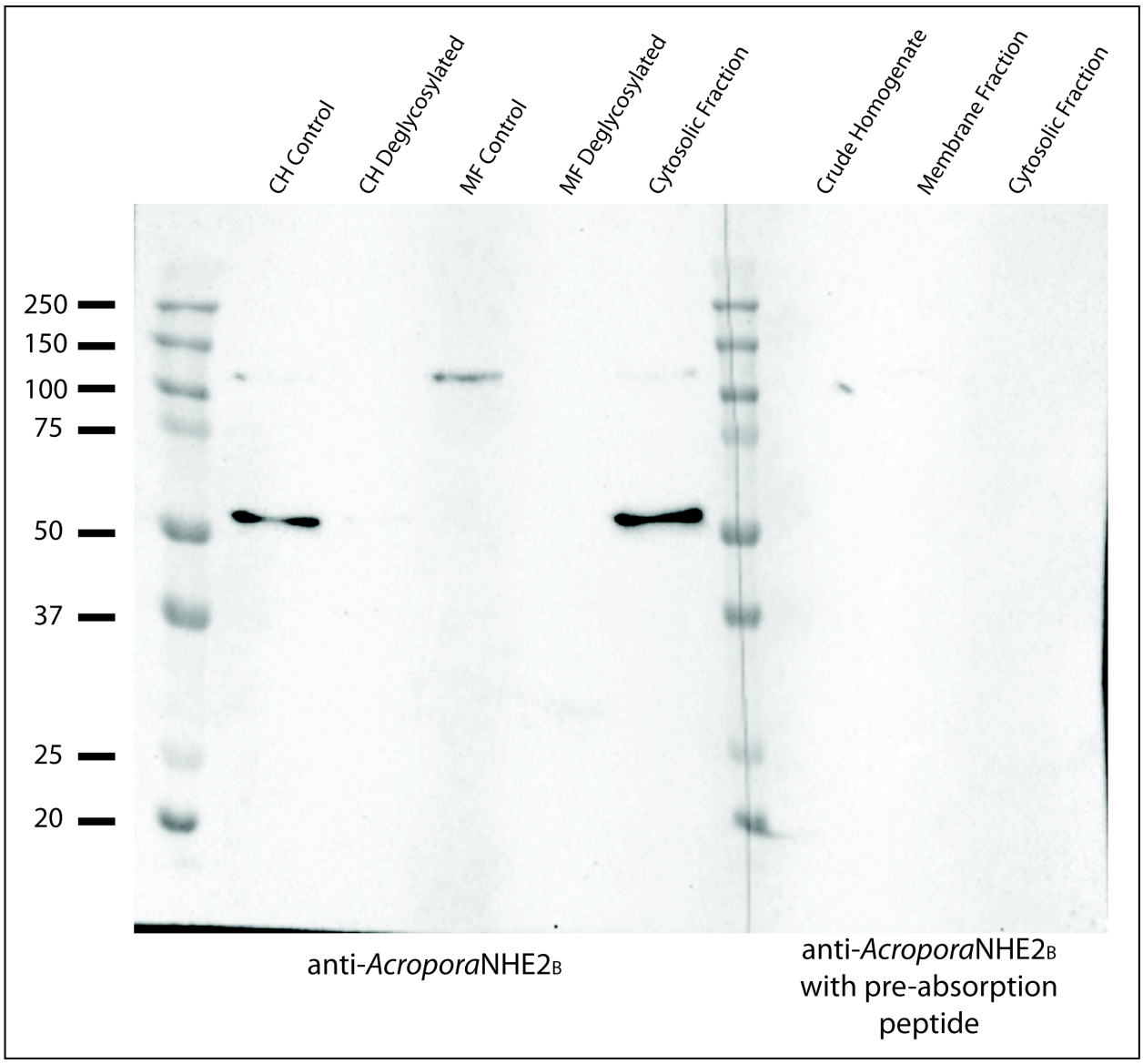

Figure 21. Optimization of anti-*Acropora*NHE$_B$ antibodies: Deglycosylation. A deglycosylation treatment was performed on two fractions, the Crude Homogenate without *Symbiodinium* and with the Membrane Fraction. The New England Biolabs Protein Mix 2 kit was used, following the denaturing conditions protocol. While the control lanes revealed the bands usually observed, the treated lanes lost all bands. The last three lanes of the membrane contained fractions that were separately treated following the preabsorption peptide control protocol described in "Methods". Each lane contains 20 µg of protein. CH= Crude Homogenate, MF= Membrane Fraction.

APPENDIX G

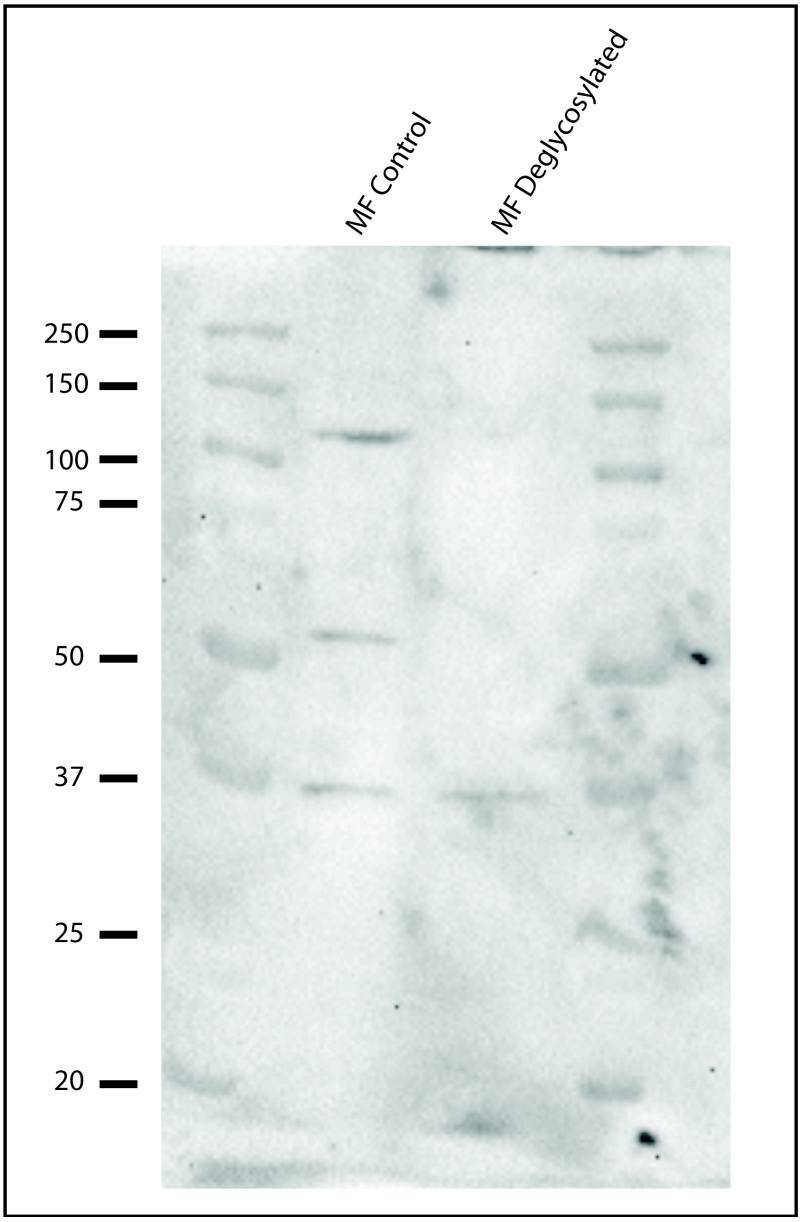

Figure 22. Optimization of anti-*Acropora*NHE$_B$ antibodies: Deglycosylation: effect of salt. Due to the high salt concentration of the S22 buffer, a different homogenization buffer was used in order to attempt to optimize the deglycosylation protocol. The Homogenization Buffer contained 100mM Tris, 1mM EDTA, 200mM NaCl, 1mM DTT, 1mM PMSF, and 10mM BHH. In order to conserve the deglycosylation enzymes, only the Membrane Fraction was used. The denaturing conditions protocol requires a 1 hr incubation at 37ºC with the deglycosylation enzymes. In order to test if *Acropora*NHE required more time to fully deglycosylate, the treated sample incubated for 4 hr incubation at 37ºC with the deglycosylation enzymes. The SDS-PAGE gel was transferred to a PVDF membrane and treated with anti-*Acorpora*NHE antibodies. The treated lane revealed no band within the predicted range. MF= Membrane Fraction.

APPENDIX H

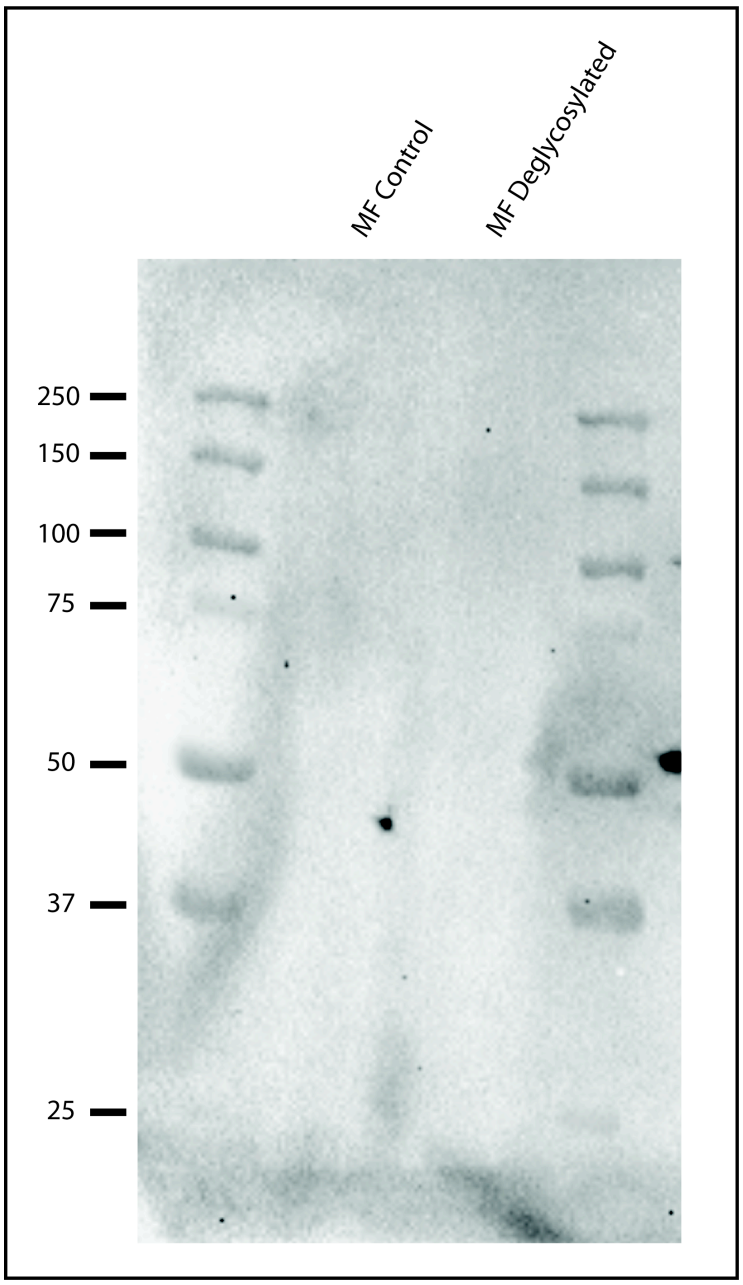

Figure 23. Optimization of anti-*Acropora*NHE$_B$ antibodies: Deglycosylation: effect of coral extract. Fetuin was suspended into the coral membrane fraction that was mixed with homogenization buffer optimized for *Acropora*NHE. In order to conserve the deglycosylation enzymes, only the Membrane Fraction was used. The SDS-PAGE gel was transferred to a PVDF membrane and treated with anti-*Acorpora*NHE antibodies. The control sample and deglycosylated sample revealed no bands. While there could still potentially be something in the coral homogenate inhibiting the reaction, it is also likely that the temperature incubations in the denaturing conditions protocol are affecting *Acropora*NHE. Further optimization is required and currently ongoing. MF= Membrane Fraction.

This thesis is being prepared for submission for publication of the material. Ortega, Mikayla; Tresguerres, Martin. Ms. Ortega was the primary investigator and author of this material.

REFERENCES

Agostini, S., Suzuki, Y., Higuchi, T., Casareto, B. E., Yoshinaga, K., Nakano, Y., & Fujimura, H. (2012). Biological and chemical characteristics of the coral gastric cavity. *Coral Reefs*, *31*(1), 147–156. https://doi.org/10.1007/s00338-011-0831-6

Al-Horani, F. A., Al-Moghrabi, S. M., & de Beer, D. (2003). Microsensor study of photosynthesis and calcification in the scleractinian coral, Galaxea fascicularis: active internal carbon cycle. *Journal of Experimental Marine Biology and Ecology*, *288*(1), 1–15. https://doi.org/10.1016/S0022-0981(02)00578-6

Alexander, R. T., Jaumouillé, V., Yeung, T., Furuya, W., Peltekova, I., Boucher, A., Zasloff, M., Orlowski, J., & Grinstein, S. (2011). Membrane surface charge dictates the structure and function of the epithelial Na+/H+ exchanger. *The EMBO Journal*, *30*(4), 679–91. https://doi.org/10.1038/emboj.2010.356

Allemand, D. (1999). Cloning of a calcium channel α1 subunit from the reef-building coral, Stylophora pistillata. *Gene*, *227*(2), 157–167. https://doi.org/10.1016/S0378-1119(98)00602-7

Allemand, D., Ferrier-Pagès, C., Furla, P., Houlbrèque, F., Puverel, S., Reynaud, S., Tambutté, É., Tambutté, S., & Zoccola, D. (2004). Biomineralisation in reef-building corals: From molecular mechanisms to environmental control. *Comptes Rendus - Palevol*, *3*(6–7 SPEC.ISS.), 453–467. https://doi.org/10.1016/j.crpv.2004.07.011

Allemand, D., Tambutté, É., Zoccola, D., & Tambutté, S. (2011). Coral Calcification, Cells to Reefs. In *Coral Reefs: An Ecosystem in Transition* (pp. 119–150). Dordrecht: Springer Netherlands. https://doi.org/10.1007/978-94-007-0114-4_9

Allison, N., Cohen, I., Finch, A. A., Erez, J., & Tudhope, A. W. (2014). Corals concentrate dissolved inorganic carbon to facilitate calcification. https://doi.org/10.1038/ncomms6741 Attaphitaya, S., Park, K., & Melvin, J. E. (1999). Molecular Cloning and Functional Expression of a Rat Na /H Exchanger (NHE5) Highly Expressed in Brain*. *The Journal of Biological Chemistry*. Retrieved from http://www.jbc.org/

Barott, K. L., Perez, S. O., Linsmayer, L. B., & Tresguerres, M. (2015a). Differential localization of ion transporters suggests distinct cellular mechanisms for calcification and photosynthesis between two coral species. *American Journal of Physiology-Regulatory, Integrative and Comparative Physiology*, *309*(3), R235–R246. https://doi.org/10.1152/ajpregu.00052.2015

Barott, K. L., Venn, A. A., Perez, S. O., Tambutté, S., & Tresguerres, M. (2015b). Coral host cells acidify symbiotic algal microenvironment to promote photosynthesis. *Proceedings of the National Academy of Sciences of the United States of America*, *112*(2), 607–12. https://doi.org/10.1073/pnas.1413483112

Basulto, A., Pérez, V. M., Noa, Y., Varela, C., Otero, A. J., & Pico, M. C. (2006). Immunohistochemical targeting of sea anemone cytolysins on tentacles, mesenteric filaments and isolated nematocysts of Stichodactyla helianthus. *Journal of Experimental Zoology Part A: Comparative Experimental Biology*, *305A*(3), 253–258. https://doi.org/10.1002/jez.a.256

Battaglino, R. A., Pham, L., Morse, L. R., Vokes, M., Sharma, A., Odgren, P. R., Sasaki, H., & Stashenko, P. (2008). NHA-oc/NHA2: a mitochondrial cation-proton antiporter selectively expressed in osteoclasts. *Bone*, *42*(1), 180–92. https://doi.org/10.1016/j.bone.2007.09.046

Beaumont, N. J., Austen, M. C., Atkins, J. P., Burdon, D., Degraer, S., Dentinho, T. P., Derous, S., Holm, P., Horton, T., van Ierland, E., Marboe, A.H., Starkey, D.J., Townsend, M., & Zarzycki, T. (2007). Identification, definition and quantification of goods and services provided by marine biodiversity: Implications for the ecosystem approach. *Marine Pollution Bulletin*, *54*(3), 253–265. https://doi.org/10.1016/J.MARPOLBUL.2006.12.003

Becker, A. M., Zhang, J., Goyal, S., Dwarakanath, V., Aronson, P. S., Moe, O. W., & Baum, M. (2007). Ontogeny of NHE8 in the rat proximal tubule. *American Journal of Physiology-Renal Physiology*, *293*(1), F255–F261. https://doi.org/10.1152/ajprenal.00400.2006

Biemesderfer, D., Reilly, R. F., Exner, M., Igarashi, P., & Aronson, P. S. (1992). Immunocytochemical characterization of Na(+)-H+ exchanger isoform NHE-1 in rabbit kidney. *The American Journal of Physiology*, *263*(5 Pt 2), F833-40. https://doi.org/10.1152/ajprenal.1992.263.5.F833

Birkeland, C. (1997). *Life and death of coral reefs*. Springer Science & Business Media.
Blom, N., Gammeltoft, S., and Brunak, S. Sequence- and structure-based prediction of eukaryotic protein phosphorylation sites. (1999). Journal of Molecular Biology: 294(5): 1351-1362.

Bookstein, C., Muschs, M. W., Depaolisti, A., Xiel, Y., Wlerealll, M., Rao, M. C., & Changs111s, E. B. (1994). A Unique Sodium-Hydrogen Exchange Isoform (NHE-4) of the Inner Medulla of the Rat Kidney Is Induced by Hyperosmolarity*. *The Journal of Biological Chemistry*, *269*(47), 29704–29709. Retrieved from http://www.jbc.org/content/269/47/29704.full.pdf

Bourgeois, S., Meer, L. Van, Wootla, B., Bloch-Faure, M., Chambrey, R., Shull, G. E., Gawenis, L.R., & Houillier, P. (2010). NHE4 is critical for the renal handling of ammonia in rodents. *Journal of Clinical Investigation*, *120*(6), 1895–1904. https://doi.org/10.1172/JCI36581

Brett, C. L., Tukaye, D. N., Mukherjee, S., & Rao, R. (2005). The Yeast Endosomal Na Exchanger Nhx1 Regulates Cellular pH to Control Vesicle Trafficking. *Molecular Biology of the Cell*, *16*, 1396–1405. https://doi.org/10.1091/mbc.E04

Brett, C. L., Wei, Y., Donowitz, M., & Rao, R. (2002). Human Na+ /H+ exchanger isoform 6 is found in recycling endosomes of cells, not in mitochondria. *American Journal of Physiology-Cell Physiology*, *282*(5), C1031–C1041. https://doi.org/10.1152/ajpcell.00420.2001

Burke, L. M., World Resources Institute., K., Spalding, M., & Perry, A. (2011). *Reefs at risk revisited*. World Resources Institute. Retrieved from http://www.vliz.be/en/imis?refid=223234

Carpenter, K. E., Abrar, M., Aeby, G., Aronson, R. B., Banks, S., Bruckner, A., Chiriboga, A., Cortés, J., Delbeek, C., DeVantier, L., Edgar, G.J., Edwards, A.J., Fenner, D., Guzmán, H.M., Hoeksema, B.W., Hodgson, G., Johan, O., Licuanan, W.Y., Livingstone, S.R., Lovell, E.R., Moore, J.A., Obura, D.O., Ochavillo, D., Polidoro, B.A., Precht, W.F., Quibilan, M.C., Reboton, C., Richards, Z.T., Rogers, A.D., Sanciangco, J., Sheppard, A., Sheppard, C., Smith, J., Stuart, S., Turak, E., Veron, J.E.N, Wallace, C., Weil, E., & Wood, E. (2008). One-third of reef-building corals face elevated extinction risk from climate change and local impacts. *Science (New York, N.Y.)*, *321*(5888), 560–3. https://doi.org/10.1126/science.1159196

Carté, B. K. (1996). Biomedical Potential of Marine Natural Products. *BioScience*, *46*(4), 271–286. https://doi.org/10.2307/1312834

Cesar, H., Lundin, C. G., Bettencourt, S., & Dixon, J. (1997). Indonesian coral reefs-An economic analysis of a precious but threatened resource. *Ambio (Sweden)*.

Chalker, B. E., & Taylor, D. L. (1975). Light-enhanced calcification, and the role of oxidative phosphorylation in calcification of the coral Acropora cervicornis. *Proceedings of the Royal Society of London. Series B, Biological Sciences*, *190*(1100), 323–31. https://doi.org/10.1098/RSPB.1975.0096

Cohen, A. L., & Holcomb, M. (2009). Why Corals Care About Ocean Acidification: Uncovering the Mechanism. *Oceanography*. Oceanography Society. https://doi.org/10.2307/24861029

Comeau, S., Carpenter, R. C., & Edmunds, P. J. (2013). Coral reef calcifiers buffer their response to ocean acidification using both bicarbonate and carbonate. *Proceedings. Biological Sciences*, *280*(1753), 20122374. https://doi.org/10.1098/rspb.2012.2374

Counillon, L., Pouyssegur, J., & Reithmeier, R. A. F. (1994). The Na+/H+ Exchanger NHE-1 Possesses N-and O-Linked Glycosylation Restricted to the First N-Terminal Extracellular Domain1'. *Biochemistry*, *33*, 10463–10469. Retrieved from https://pubs.acs.org/doi/pdf/10.1021/bi00200a030

Davy, S. K., Allemand, D., & Weis, V. M. (2012). Cell biology of cnidarian-dinoflagellate symbiosis. *Microbiology and Molecular Biology Reviews : MMBR*, *76*(2), 229–61. https://doi.org/10.1128/MMBR.05014-11

Diering, G. H., Mills, F., Bamji, S. X., & Numata, M. (2011). Regulation of dendritic spine growth through activity-dependent recruitment of the brain-enriched Na+ /H+ exchanger NHE5.

Molecular Biology of the Cell, *22*(13), 2246–2257. https://doi.org/10.1091/mbc.e11-01-0066

Dixon, J. A., Fallon Scura, L., & van't Hof, T. (1993). Meeting ecological and economic goals: marine parks in the Caribbean. *Ambio (Sweden)*.

Dodge, R. E., & Gilbert, T. R. (1984). Chronology of lead pollution contained in banded coral skeletons. *Marine Biology*, *82*(1), 9–13. https://doi.org/10.1007/BF00392758

Donowitz, M., & Li, X. (2007). Regulatory Binding Partners and Complexes of NHE3. *Physiological Reviews*, *87*(3), 825–872. https://doi.org/10.1152/physrev.00030.2006

Donowitz, M., Ming Tse, C., & Fuster, D. (2013). SLC9/NHE gene family, a plasma membrane and organellar family of Na+/H+ exchangers. *Molecular Aspects of Medicine*, *34*(2–3), 236–251. https://doi.org/10.1016/J.MAM.2012.05.001

Eakin, C. M., McManus, J. W., Spalding, M. D., & Jameson, S. C. (1997). Coral reef status around the world: where are we and where do we go from here. In *Proceedings of the 8th International Coral Reef Symposium* (Vol. 1, pp. 277-282).

Eisenhauer, A., Wasserburg, G. J., Chen, J. H., Bonani, G., Collins, L. B., Zhu, Z. R., & Wyrwoll, K. H. (1993). Holocene sea-level determination relative to the Australian continent: U/Th (TIMS) and 14C (AMS) dating of coral cores from the Abrolhos Islands. *Earth and Planetary Science Letters*, *114*(4), 529–547. https://doi.org/10.1016/0012-821X(93)90081-J

Eladari, D., & Chambrey, R. (2010). Ammonium transport in the kidney. *Journal of Nephrology*, *23 Suppl 16*, S28-34. Retrieved from http://www.ncbi.nlm.nih.gov/pubmed/21170885

Evans, D. H., Piermarini, P. M., & Choe, K. P. (2005). The Multifunctional Fish Gill: Dominant Site of Gas Exchange, Osmoregulation, Acid-Base Regulation, and Excretion of Nitrogenous Waste. *Physiological Reviews*, *85*(1), 97–177. https://doi.org/10.1152/physrev.00050.2003

Falkowski, P. G., Dubinsky, Z., Muscatine, L., & Porter, J. W. (1984). Light and the Bioenergetics of a Symbiotic Coral. *BioScience*, *34*(11), 705–709. https://doi.org/10.2307/1309663

Feizi, T. (1993). Oligosaccharides that mediate mammalian cell-cell adhesion. *Current Opinion in Structural Biology*, *3*(5), 701–710. https://doi.org/10.1016/0959-440X(93)90053-N

Fliegel, L., & Fröhlich, O. (1993). The Na+/H+ exchanger: an update on structure, regulation and cardiac physiology. *The Biochemical Journal*, *296 (Pt 2)*(Pt 2), 273–85. Retrieved from http://www.ncbi.nlm.nih.gov/pubmed/8257412

Furla P, Galgan I, Durand I, A. D. (2000). Carbon sources for coral calcification and photosynthesis. *The Journal of Experimental Biology*, *203*, 3445–3457. Retrieved from http://jeb.biologists.org/content/jexbio/203/22/3445.full.pdf

Fuster, D. G., Zhang, J., Shi, M., Bobulescu, I. A., Andersson, S., & Moe, O. W. (2008).

Characterization of the sodium/hydrogen exchanger NHA2. *Journal of the American Society of Nephrology : JASN*, *19*(8), 1547–56. https://doi.org/10.1681/ASN.2007111245

Galloway, S. B., Woodley, C. M., McLaughlin, S. M., Work, T. M., Bochsler, V. S., Meteyer, C. U., … Reynolds, T. L. (2007). Coral Disease and Health Workshop: Coral Histopathology II. Retrieved from http://aquaticcommons.org/2236/

Gawenis, L. R., Greeb, J. M., Prasad, V., Grisham, C., Sanford, L. P., Doetschman, T., Andringa, A., Miller, M.L., & Shull, G. E. (2005). Impaired gastric acid secretion in mice with a targeted disruption of the NHE4 Na+/H+ exchanger. *The Journal of Biological Chemistry*, *280*(13), 12781–9. https://doi.org/10.1074/jbc.M414118200

Goldberg, W. M. (2002). Feeding behavior, epidermal structure and mucus cytochemistry of the scleractinian Mycetophyllia reesi, a coral without tentacles. *Tissue and Cell*, *34*(4), 232–245. https://doi.org/10.1016/S0040-8166(02)00009-5

Goreau, T. F. (1959). The Physiology of Skeleton Formation in Corals. I. A Method for Measuring the Rate of Calcium Deposition by Corals Under Different Conditions. *The Biological Bulletin, 116*(1), 59-75. https://doi.org/10.2307/1539156

Guest, J. R., Dizon, R. M., Edwards, A. J., Franco, C., & Gomez, E. D. (2011). How Quickly do Fragments of Coral "Self-Attach" after Transplantation? *Restoration Ecology*, *19*(2), 234–242. https://doi.org/10.1111/j.1526-100X.2009.00562.x

Gupta, R., Jung, E. & Brunak, S. In preparation, (2004). Prediction of N-glycosylation sites in human proteins.

Hamby, S.E. & Hirst, J.D. (2008). Prediction of Glycosylation Sites Using Random Forests. BMC Bioinformatics, 9, 500. DOI: http://dx.doi.org/10.1186/1471-2105-9-500

Hamm, L. L., Nakhoul, N., & Hering-Smith, K. S. (2015). Acid-Base Homeostasis. *Clinical Journal of the American Society of Nephrology : CJASN*, *10*(12), 2232–42. https://doi.org/10.2215/CJN.07400715

Hoogerwerf, W. A., Tsao, S. C., Devuyst, O., Levine, S. A., Yun, C. H., Yip, J. W., Cohen, M.E., Wilson, P.D., Lazenby, A.J., Tse, C., & Donowitz, M. (1996). NHE2 and NHE3 are human and rabbit intestinal brush-border proteins. *The American Journal of Physiology*, *270*(1 Pt 1), G29-41. https://doi.org/10.1152/ajpgi.1996.270.1.G29

Hosey, M. M., & Lazdunski, M. (1988). Calcium Channels: Molecular Pharmacology, Structure and Regulation. *J. Membrane Biol*, *104*, 81–105. Retrieved from https://link.springer.com/content/pdf/10.1007/BF01870922.pdf

Howard, L. S., & Brown, B. E. (1984). Heavy metals and reef corals. *Oceanogr. Mar. Biol. Ann. Rev*, *22*, 195-210.

Hu, N.-J., Iwata, S., Cameron, A. D., & Drew, D. (2011). Crystal structure of a bacterial homologue of the bile acid sodium symporter ASBT. *Nature*, *478*(7369), 408–411. https://doi.org/10.1038/nature10450

Ikeda, T., Schmitt, B., Pouyssegur, J., Wakabayashi, S., & Shigekawa, M. (1997). Identification of cytoplasmic subdomains that control pH-sensing of the Na+/H+ exchanger (NHE1): pH-maintenance, ATP-sensitive, and flexible loop domains. *The Journal of Biochemistry*, *121*(2), 295-303.

Johnston, I. S. (1980). The Ultrastructure of Skeletogenesis in Hermatypic Corals. *International Review of Cytology*, *67*, 171–214. https://doi.org/10.1016/S0074-7696(08)62429-8

Jokiel, P. L. (2013). Coral reef calcification: carbonate, bicarbonate and proton flux under conditions of increasing ocean acidification. *Proceedings. Biological Sciences*, *280*(1764), 20130031. https://doi.org/10.1098/rspb.2013.0031

Jokiel, P. L. (2011). The reef coral two compartment proton flux model: A new approach relating tissue-level physiological processes to gross corallum morphology. *Journal of Experimental Marine Biology and Ecology*, *409*(1-2), 1-12.

Kang'ethe, W., Aimanova, K. G., Pullikuth, A. K., & Gill, S. S. (2007). NHE8 mediates amiloride-sensitive Na+/H+ exchange across mosquito Malpighian tubules and catalyzes Na+ and K+ transport in reconstituted proteoliposomes. *American Journal of Physiology-Renal Physiology*, *292*(5), F1501–F1512. https://doi.org/10.1152/ajprenal.00487.2005

Karmazyn, M., Liu, Q., Gan, X. T., Brix, B. J., & Fliegel, L. (2003). Aldosterone increases NHE-1 expression and induces NHE-1-dependent hypertrophy in neonatal rat ventricular myocytes. *Hypertension (Dallas, Tex. : 1979)*, *42*(6), 1171–6. https://doi.org/10.1161/01.HYP.0000102863.23854.0B

Kelley, L. A., Mezulis, S., Yates, C. M., Wass, M. N., & Sternberg, M. J. (2015). The Phyre2 web portal for protein modeling, prediction and analysis. *Nature protocols*, *10*(6), 845.

Kearse, M., Moir, R., Wilson, A., Stones-Havas, S., Cheung, M., Sturrock, S., Buxton, S., Cooper, A., Markowitz, S., Duran, C., Thierer, T., Ashton, B., Mentjies, P., & Drummond, A. (2012). Geneious Basic: an integrated and extendable desktop software platform for the organization and analysis of sequence data.*Bioinformatics*, *28*(12), 1647-1649.

Laurent, J., Venn, A., Tambutté, É., Ganot, P., Allemand, D., & Tambutté, S. (2014). Regulation of intracellular pH in cnidarians: response to acidosis in *Anemonia viridis*. *FEBS Journal*, *281*(3), 683–695. https://doi.org/10.1111/febs.12614

Lesser, M. P., Mazel, C. H., Gorbunov, M. Y., & Falkowski, P. G. (2004). Discovery of symbiotic nitrogen-fixing cyanobacteria in corals. *Science (New York, N.Y.)*, *305*(5686), 997–1000. https://doi.org/10.1126/science.1099128

Madshus, I. H. (1988). Regulation of intracellular pH in eukaryotic cells. *Biochem. J*, *250*, 1–8. Retrieved from https://www.ncbi.nlm.nih.gov/pmc/articles/PMC1148806/pdf/biochemj00237-0011.pdf

Marshall, A. T. (1996). Calcification in Hermatypic and Ahermatypic Corals. *Science*, *271*(5249), 637–639. https://doi.org/10.1126/science.271.5249.637

Mass, T., Drake, J. L., Haramaty, L., Kim, J. D., Zelzion, E., Bhattacharya, D., & Falkowski, P. G. (2013). Cloning and Characterization of Four Novel Coral Acid-Rich Proteins that Precipitate Carbonates In Vitro. *Current Biology*, *23*(12), 1126–1131. https://doi.org/10.1016/J.CUB.2013.05.007

Mass, T., Giuffre, A. J., Sun, C.-Y., Stifler, C. A., Frazier, M. J., Neder, M., Tamura, N., Stan, C.V., Marcus, M.A., & Gilbert, P. U. P. A. (2017). Amorphous calcium carbonate particles form coral skeletons. *Proceedings of the National Academy of Sciences of the United States of America*, *114*(37), E7670–E7678. https://doi.org/10.1073/pnas.1707890114

McLachlin, D. T., & Chait, B. T. (2001). Analysis of phosphorylated proteins and peptides by mass spectrometry. *Current Opinion in Chemical Biology*, *5*(5), 591–602. https://doi.org/10.1016/S1367-5931(00)00250-7

Miyazaki, E., Sakaguchi, M., Wakabayashi, S., Shigekawa, M., & Mihara, K. (2001). NHE6 protein possesses a signal peptide destined for endoplasmic reticulum membrane and localizes in secretory organelles of the cell. *Journal of Biological Chemistry*.

Moberg, F., & Folke, C. (1999). Ecological goods and services of coral reef ecosystems. *Ecological Economics*, *29*, 215–233. Retrieved from http://citeseerx.ist.psu.edu/viewdoc/download?doi=10.1.1.487.5715&rep=rep1&type=pdf

Moya, A., Tambutté, S., Bertucci, A., Tambutté, E., Lotto, S., Vullo, D., Supuran, C.T., Allemand, D., & Zoccola, D. (2008). Carbonic anhydrase in the scleractinian coral Stylophora pistillata: characterization, localization, and role in biomineralization. *The Journal of Biological Chemistry*, *283*(37), 25475–84. https://doi.org/10.1074/jbc.M804726200

Nakamura, N., Tanaka, S., Teko, Y., Mitsui, K., & Kanazawa, H. (2005). Four Na+/H+ exchanger isoforms are distributed to Golgi and post-Golgi compartments and are involved in organelle pH regulation. *The Journal of Biological Chemistry*, *280*(2), 1561–72. https://doi.org/10.1074/jbc.M410041200

Numata, M., & Orlowski, J. (2001). Molecular cloning and characterization of a novel (Na+,K+)/H+ exchanger localized to the trans-Golgi network. *The Journal of Biological Chemistry*, *276*(20), 17387–94. https://doi.org/10.1074/jbc.M101319200

Ogden, J. C. (1988). The influence of adjacent systems on the structure and function of coral reefs. In *Proceedings of the International Coral Reef Symp* (Vol. 1, pp. 123-129).

Orlowski, J., & Grinstein, S. (1997). Na+/H+ exchangers of mammalian cells. *The Journal of Biological Chemistry*, *272*(36), 22373–6. https://doi.org/10.1074/JBC.272.36.22373

Phillips, J. H. (1963). Immune mechanisms in the phylum Coelenterata. *The Lower Metazoa*, 425-431.

Putnam, H. M., Davidson, J. M., & Gates, R. D. (2016). Ocean acidification influences host DNA methylation and phenotypic plasticity in environmentally susceptible corals. *Evolutionary Applications*, *9*(9), 1165–1178. https://doi.org/10.1111/eva.12408

Putnam, R. W., & Roos, A. (1997). Intracellular pH. *Handbook of physiology*, *14*, 389-440.

Rasmussen, J. R. (1992). Effect of glycosylation on protein function. *Current Opinion in Structural Biology*, *2*(5), 682–686. https://doi.org/10.1016/0959-440X(92)90201-H

Richmond, R. H. (1993). Coral reefs: Present problems and future concerns resulting from anthropogenic disturbance. *Integrative and Comparative Biology*, *33*(6), 524–536. https://doi.org/10.1093/icb/33.6.524

Ries, J. B. (2011). A physicochemical framework for interpreting the biological calcification response to CO 2 -induced ocean acidification. https://doi.org/10.1016/j.gca.2011.04.025

Rohwer, F., Seguritan, V., Azam, F., & Knowlton, N. (2002). Diversity and distribution of coral-associated bacteria. *Marine Ecology Progress Series*, *243*, 1–10. https://doi.org/10.3354/meps243001

Romano, S. L., & Cairns, S. D. (2000). Molecular phylogenetic hypotheses for the evolution of scleractinian corals. *Bulletin of Marine Science*, *67*(3), 1043-1068.

Romano, S. L., & Palumbi, S. R. (1996). Evolution of Scleractinian Corals Inferred from Molecular Systematics. *Science*, *271*(5249), 640–642. https://doi.org/10.1126/science.271.5249.640

Runnalls, L. A., & Coleman, M. L. (2003). Record of natural and anthropogenic changes in reef environments (Barbados West Indies) using laser ablation ICP-MS and sclerochronology on coral cores. *Coral Reefs*, *22*(4), 416–426. https://doi.org/10.1007/s00338-003-0349-7

Sangan, P., Rajendran, V. M., Geibel, J. P., & Binder, H. J. (2002). Cloning and expression of a

chloride-dependent Na+-H+ exchanger. *The Journal of Biological Chemistry*, *277*(12), 9668–75. https://doi.org/10.1074/jbc.M110852200

Simonin, A., & Fuster, D. (2010). Nedd4-1 and beta-arrestin-1 are key regulators of Na+/H+ exchanger 1 ubiquitylation, endocytosis, and function. *The Journal of Biological Chemistry*, *285*(49), 38293–303. https://doi.org/10.1074/jbc.M110.115089

Smith, S. V. (1978). Coral-reef area and the contributions of reefs to processes and resources of the world's oceans. *Nature*, *273*(May), 225–226. https://doi.org/10.1038/273225a0

Soleimani, M., Singh, G., Bookstein, C., Rao, M. C., Chang, E. B., & Dominguez, J. H. (1996). Inhibition of glycosylation decreases Na+/H+ exchange activity, blocks NHE-3 transport to the membrane, and increases NHE-3 mRNA expression in LLC-PK1 cells. *Journal of Laboratory and Clinical Medicine*, *127*(6), 565–573. https://doi.org/10.1016/S0022-2143(96)90147-X

Sorokin, Y. I. (2013). *Coral reef ecology* (Vol. 102). Springer Science & Business Media.

Steentoft C, Vakhrushev SY, Joshi HJ, Kong Y, Vester-Christensen MB, Schjoldager KT, Lavrsen K, Dabelsteen S, Pedersen NB, Marcos-Silva L, Gupta R, Bennett EP, Mandel U, Brunak S, Wandall HH, Levery SB, Clausen H. (2013). Precision mapping of the human O-GalNAc glycoproteome through SimpleCell technology. EMBO J, 32(10):1478-88 (doi: 10.1038/emboj.2013.79. Epub 2013 Apr 12)

Stolarski, J., Kitahara, M. V, Miller, D. J., Cairns, S. D., Mazur, M., & Meibom, A. (2011). The ancient evolutionary origins of Scleractinia revealed by azooxanthellate corals. *BMC Evolutionary Biology*, *11*(1), 316. https://doi.org/10.1186/1471-2148-11-316

Subramanya, S. B., Rajendran, V. M., Srinivasan, P., Nanda Kumar, N. S., Ramakrishna, B. S., & Binder, H. J. (2007). Differential regulation of cholera toxin-inhibited Na-H exchange isoforms by butyrate in rat ileum. *American Journal of Physiology-Gastrointestinal and Liver Physiology*, *293*(4), G857–G863. https://doi.org/10.1152/ajpgi.00462.2006

Tambutté, É., Allemand, D., Mueller, E., & Jaubert, J. (1996). A Compartmental Approach To The Mechanism of Calcification in Hermatypic Corals. *The Journal of Experimental Biology*, *199*, 1029–1041. Retrieved from http://jeb.biologists.org/content/jexbio/199/5/1029.full.pdf

Tambutté, E., Allemand, D., Zoccola, D., Meibom, A., Lotto, S., Caminiti, N., & Tambutté, S. (2007). Observations of the tissue-skeleton interface in the scleractinian coral Stylophora pistillata. *Coral Reefs*, *26*(3), 517–529. https://doi.org/10.1007/s00338-007-0263-5
Tresguerres, M., Barott, K. L., Barron, M. E., Deheyn, D. D., Kline, D. I., & Linsmayer, L. B. (2017). Cell Biology of Reef-Building Corals: Ion Transport, Acid/Base Regulation, and Energy Metabolism. In *Acid-Base Balance and Nitrogen Excretion in Invertebrates* (pp. 193–218). Cham: Springer International Publishing. https://doi.org/10.1007/978-3-319-39617-0_7

Tse, C.-M., Levine, S. A., Yun, C. H. C., Khurana, S., & Donowitz, M. (1994). Na+/H+ Exchanger-2 Is an O-Linked but Not an N-Linked Sialoglycoprotein*. *Biochemistry*, *33*, 12954–

12961. Retrieved from https://pubs.acs.org/doi/pdf/10.1021/bi00248a003

Venn, A. A., Tambutté, E., Holcomb, M., Laurent, J., Allemand, D., & Tambutté, S. (2013). Impact of seawater acidification on pH at the tissue-skeleton interface and calcification in reef corals. *Proceedings of the National Academy of Sciences of the United States of America*, *110*(5), 1634–9. https://doi.org/10.1073/pnas.1216153110

Venn, A., Tambutté, E., Holcomb, M., Allemand, D., & Tambutté, S. (2011). Live Tissue Imaging Shows Reef Corals Elevate pH under Their Calcifying Tissue Relative to Seawater. *PLoS ONE*, *6*(5), e20013. https://doi.org/10.1371/journal.pone.0020013

Veron, J. E. N. (1993). Corals of Australia and the Indo-pacific.

Wang, D., King, S. M., Quill, T. A., Doolittle, L. K., & Garbers, D. L. (2003). A new sperm-specific Na+/H+ Exchanger required for sperm motility and fertility. *Nature Cell Biology*, *5*(12), 1117–1122. https://doi.org/10.1038/ncb1072

Wegley, L., Yu, Y.N., Breitbart, M., Casas, V., Kline, D.I., Rohwer, F. (2003) Coral-associated archaea. Marine Ecology-Progress Series. 273:89-96.

Wijsman-Best, M. (1977). Intra-and extratentacular budding in hermatypic reef corals. In *Proc. 3rd Int. Coral Reef Symp* (Vol. 1, pp. 471-475).

Wilkinson, C. (1993). Coral reefs are facing widespread devastation. In *Proceedings of the 7th International Coral Reef Symposium* (pp. 11-12).

Woo, A. L., James, P. F., & Lingrel, J. B. (2002). Roles of the Na,K-ATPase a4 Isoform and the Na þ /H þ Exchanger in Sperm Motility. *Molecular Reproduction and Development, 62*, 348–356. https://doi.org/10.1002/mrd.90002

Xiang, M., Feng, M., Muend, S., & Rao, R. (2007). A human Na+/H+ antiporter sharing evolutionary origins with bacterial NhaA may be a candidate gene for essential hypertension. *Proceedings of the National Academy of Sciences of the United States of America*, *104*(47), 18677–81. https://doi.org/10.1073/pnas.0707120104

Xu, H., Ghishan, F. K., & Kiela, P. R. (2018). SLC9 Gene Family: Function, Expression, and Regulation. In *Comprehensive Physiology* (Vol. 8, pp. 555–583). Hoboken, NJ, USA: John Wiley & Sons, Inc. https://doi.org/10.1002/cphy.c170027
Xue, L., Aihara, E., Wang, T. C., & Montrose, M. H. (2011). Trefoil factor 2 requires Na/H exchanger 2 activity to enhance mouse gastric epithelial repair. *The Journal of Biological Chemistry*, *286*(44), 38375–82. https://doi.org/10.1074/jbc.M111.268219

Zoccola, D., Tambutté, E., Kulhanek, E., Puverel, S., Scimeca, J.-C., Allemand, D., & Tambutté, S. (2004). Molecular cloning and localization of a PMCA P-type calcium ATPase from the coral Stylophora pistillata. *Biochimica et Biophysica Acta (BBA) - Biomembranes*, *1663*(1–2), 117–

126. https://doi.org/10.1016/J.BBAMEM.2004.02.010

Zoccola, D., Tambutté, E., Sénégas-Balas, F., Michiels, J.-F., Failla, J.-P., Jaubert, J., &